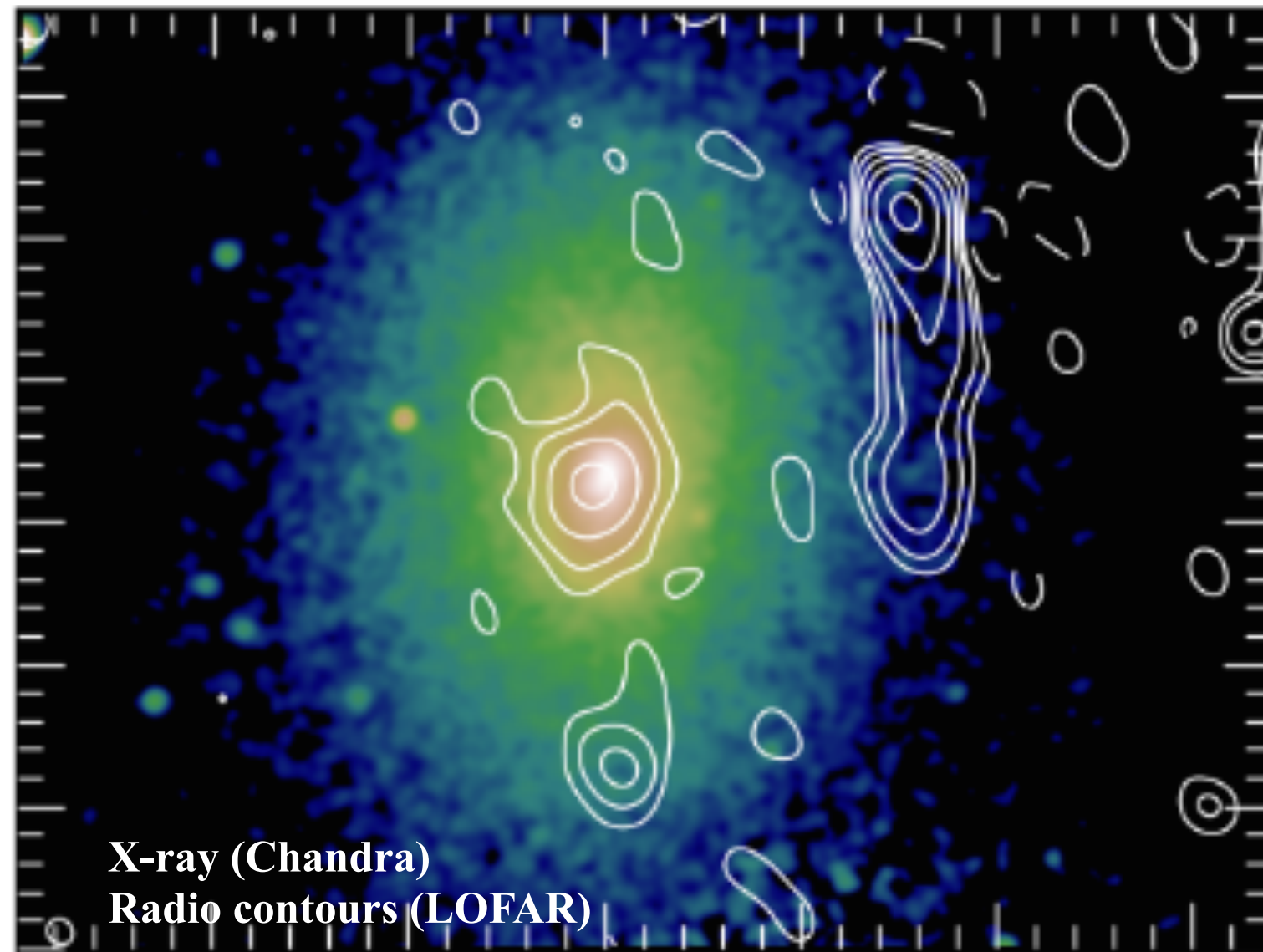


New LOFAR detection in the galaxy cluster A1413

Connection between non-thermal and thermal emission

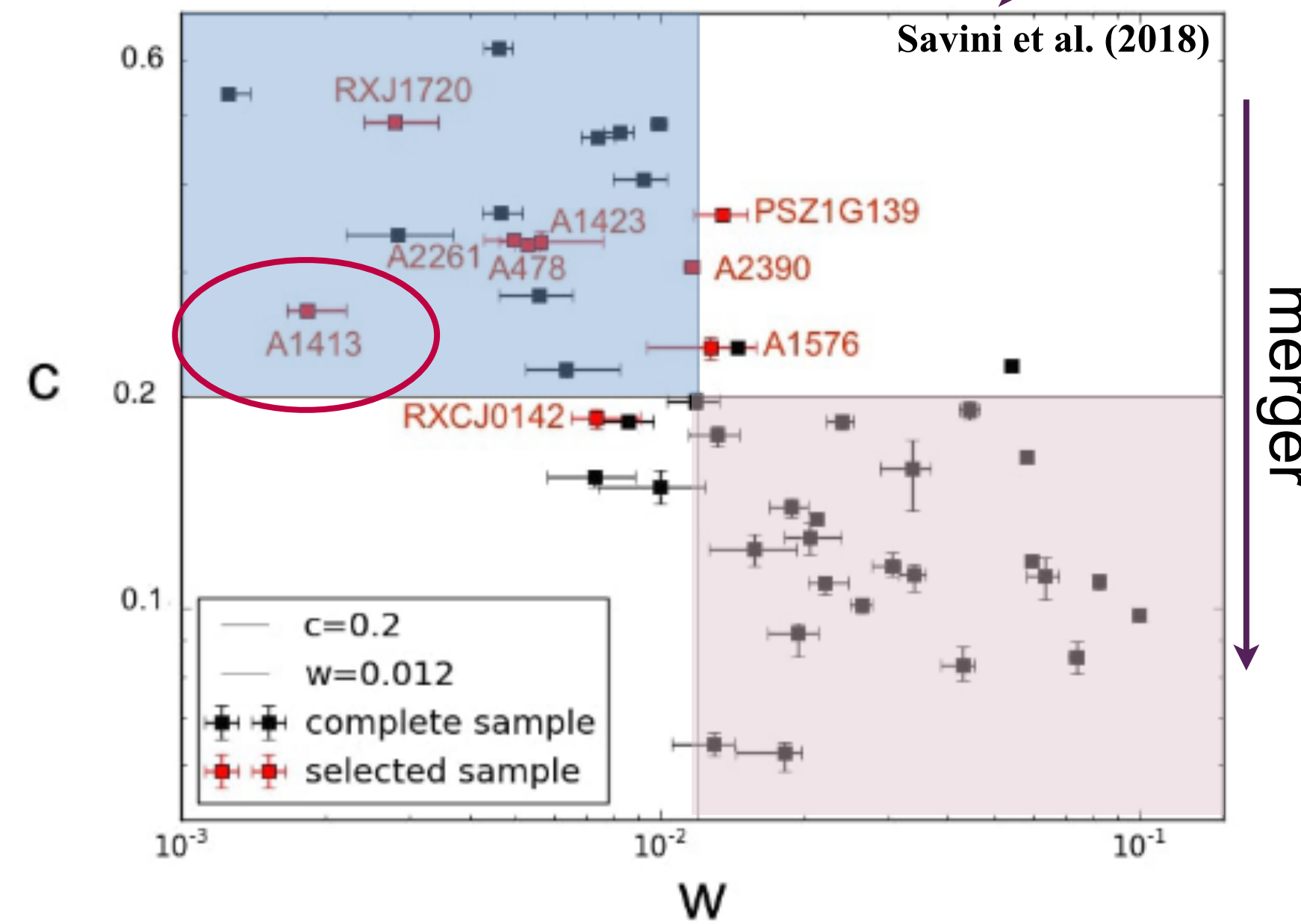
Collaboration with **CHEX-MATE** and **LoTSS**

The galaxy cluster Abell 1413: a multi-wavelengths analysis

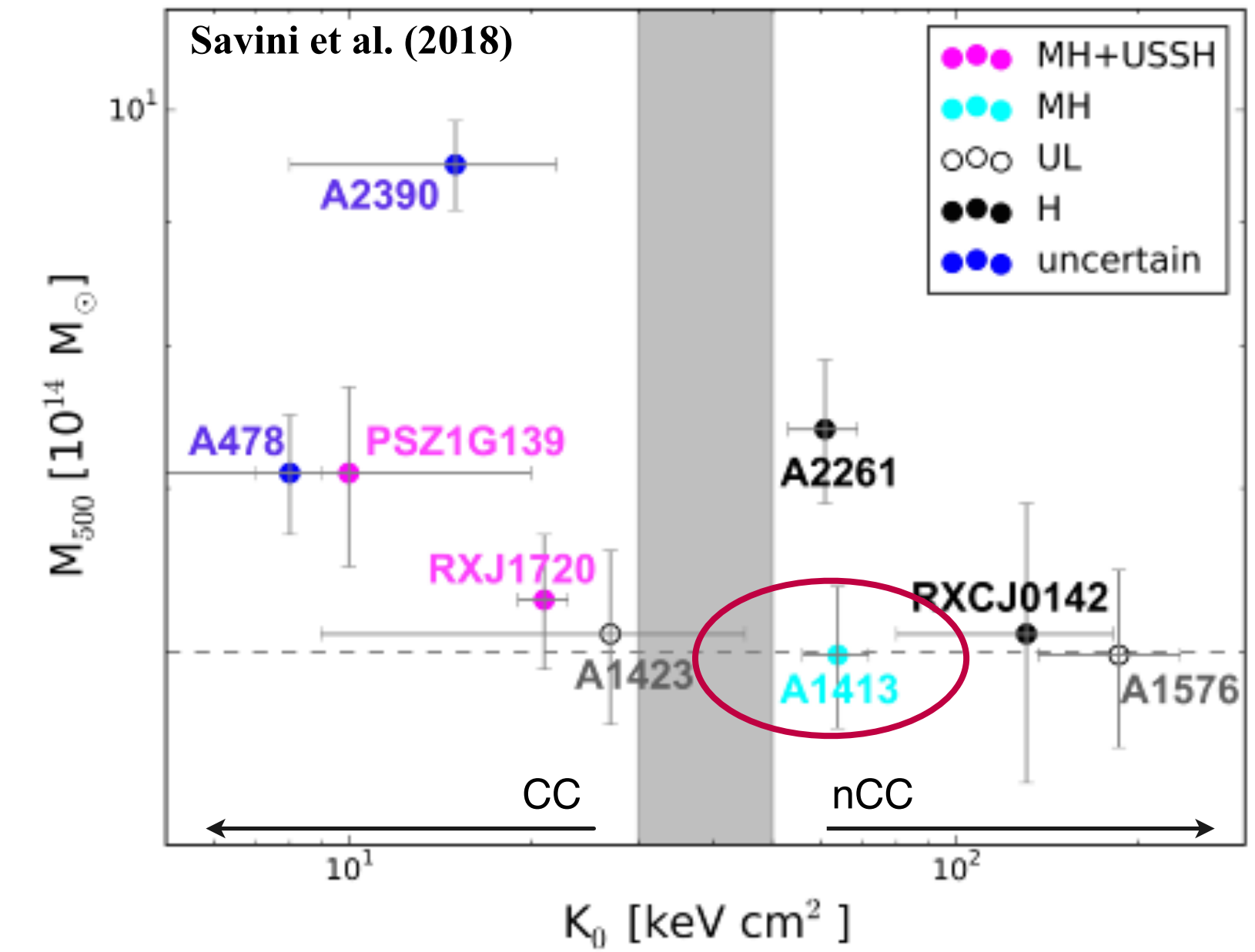


Savini et al. (2018)

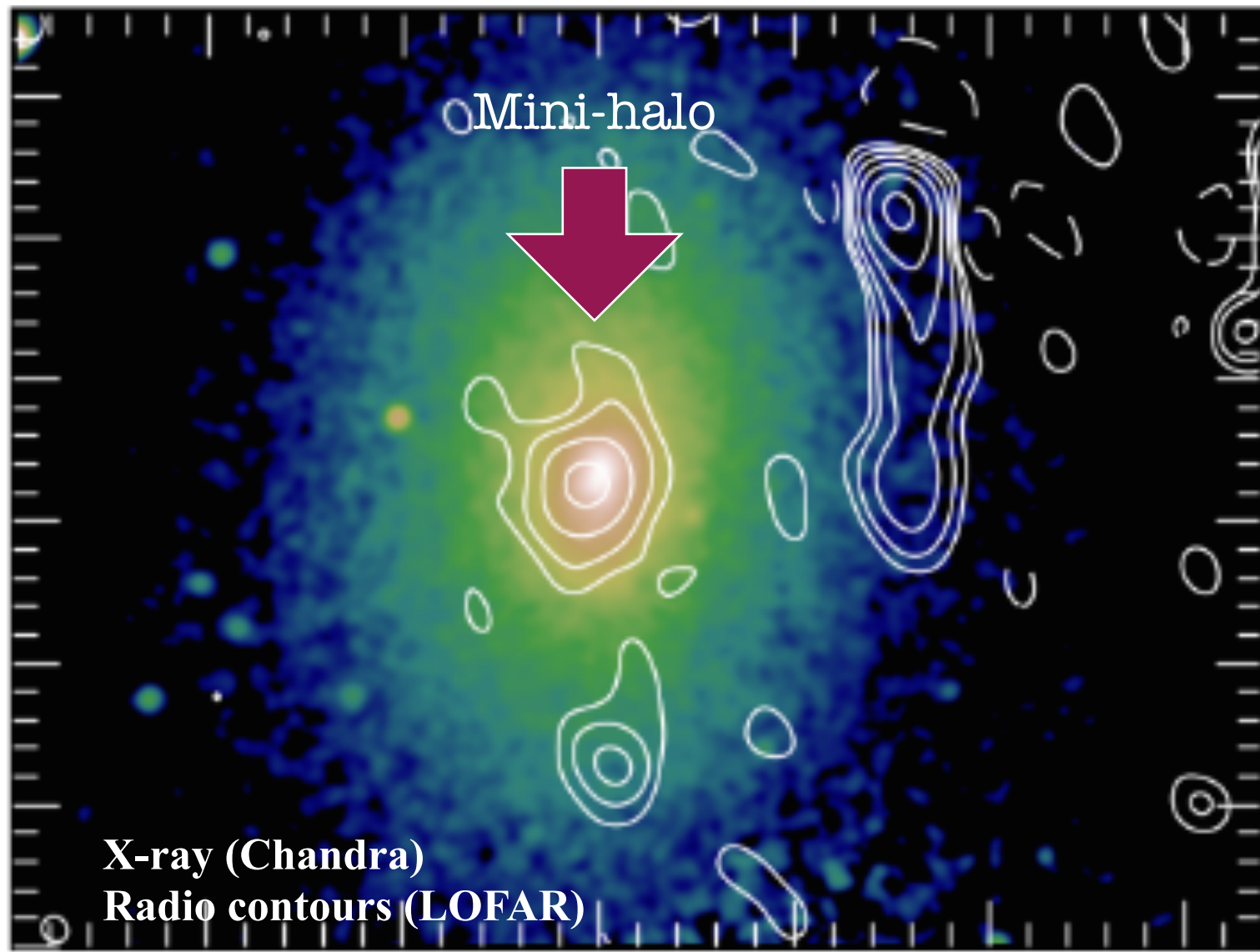
Merging vs non merging merger



CoolCore vs non CoolCore

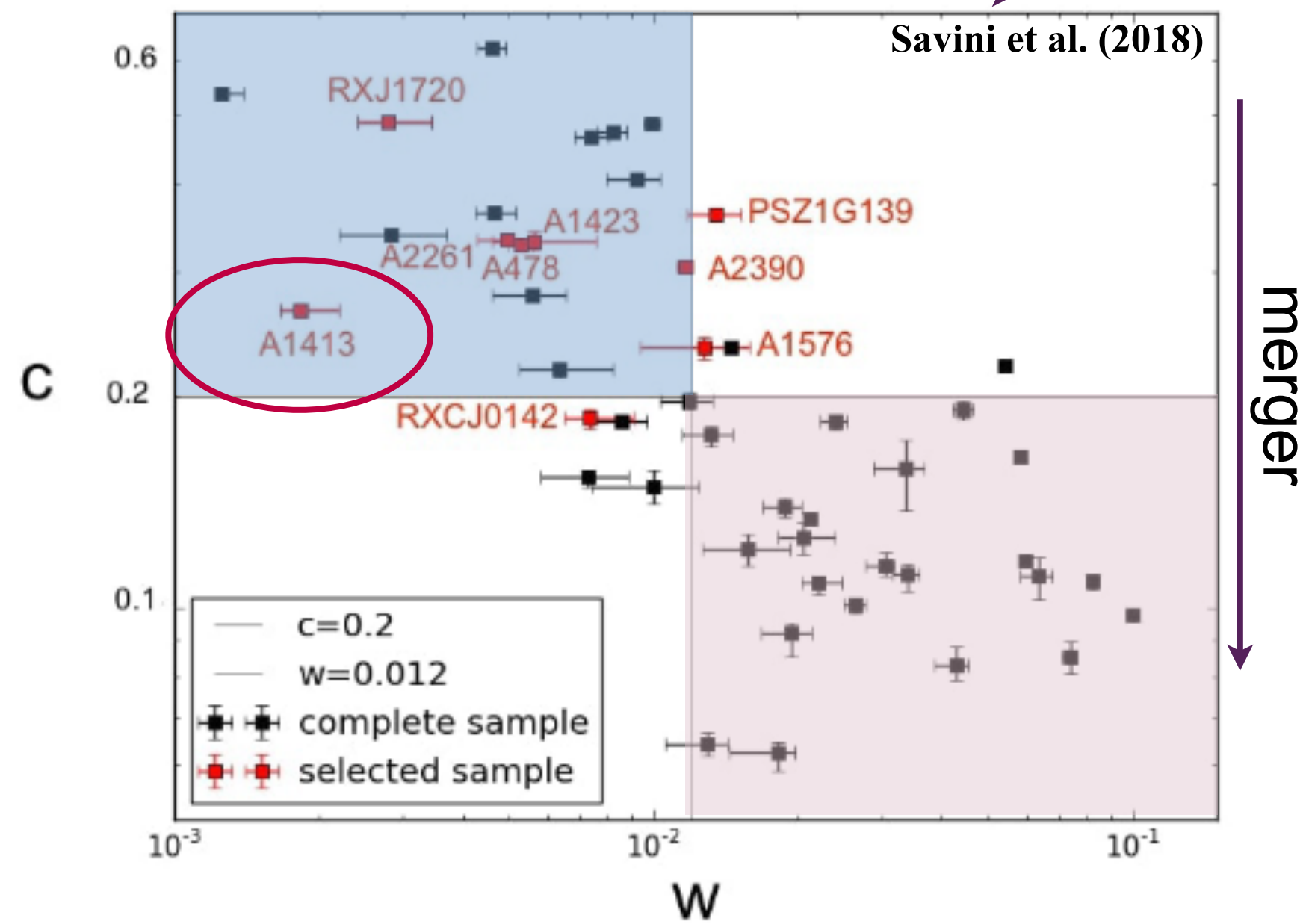


The galaxy cluster Abell 1413: a multi-wavelengths analysis

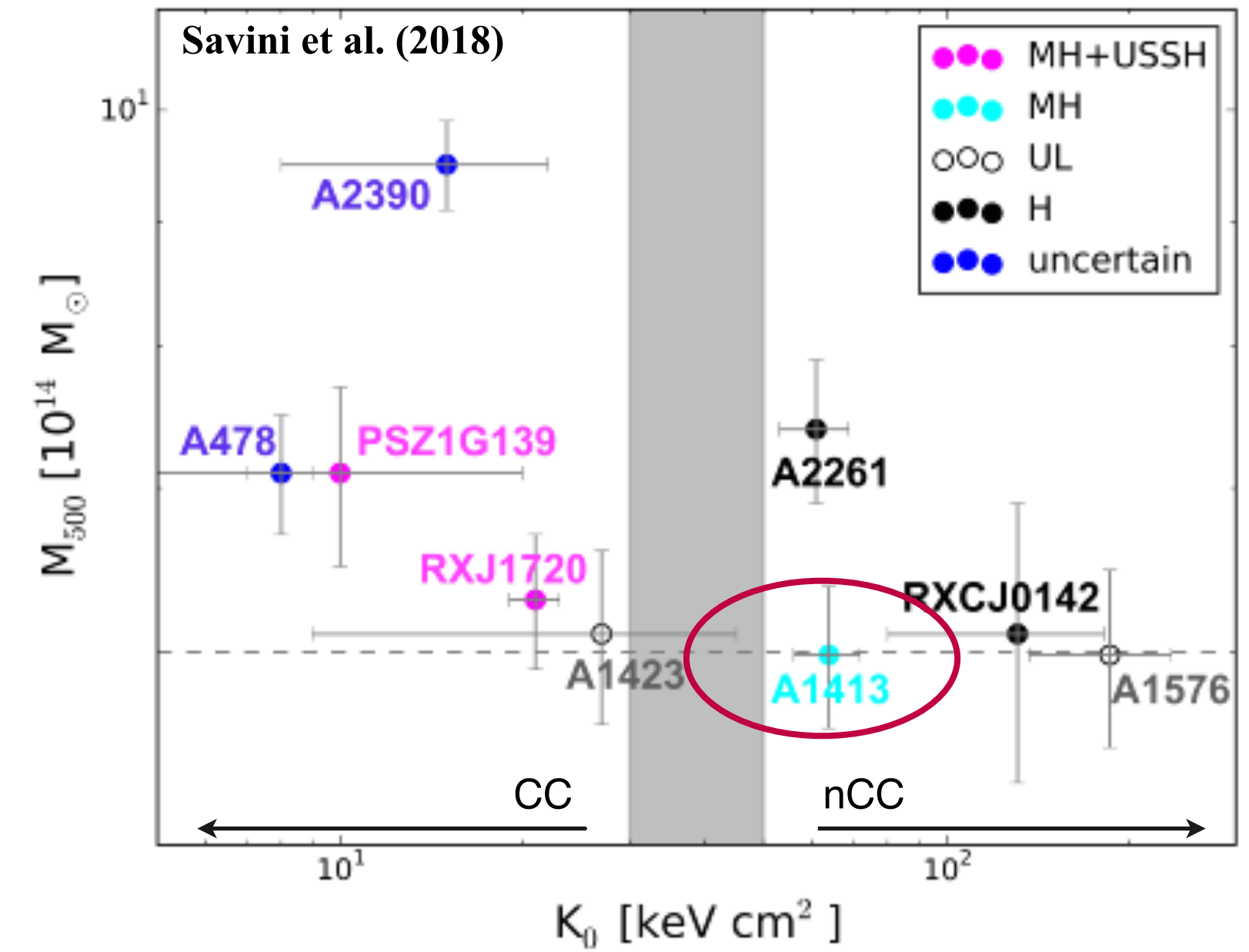


Savini et al. (2018)

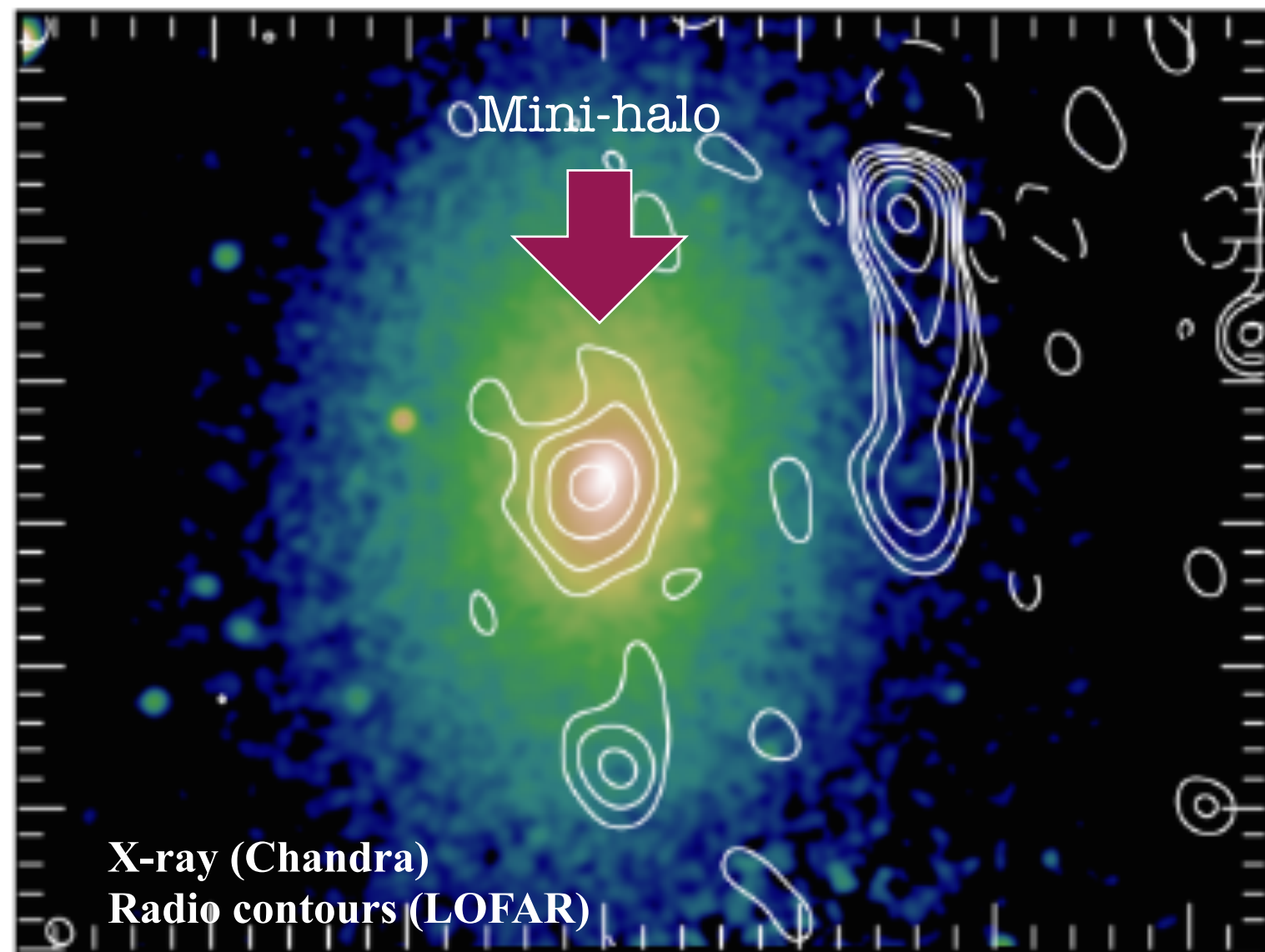
Merging vs non merging merger



CoolCore vs non CoolCore

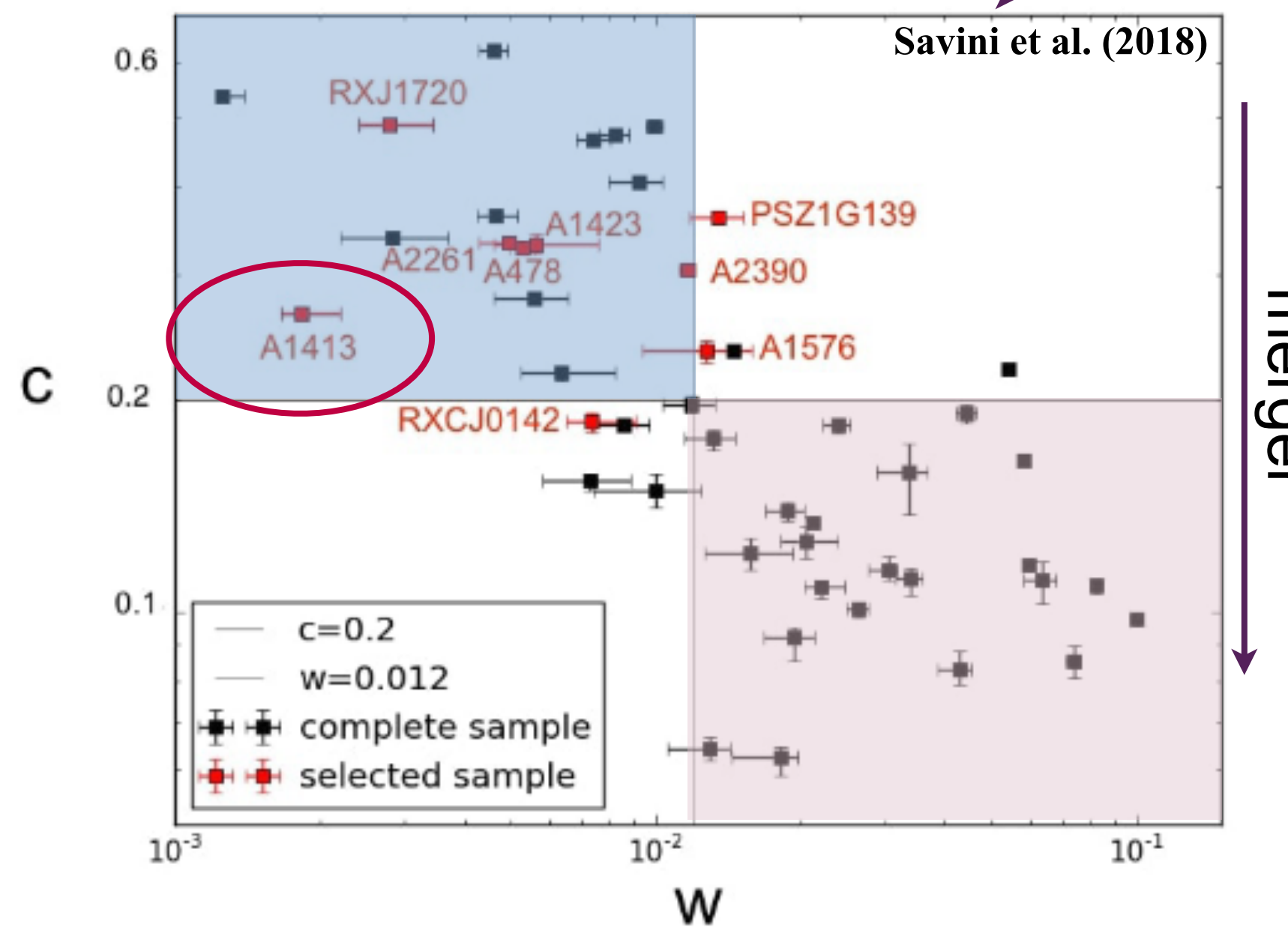


The galaxy cluster Abell 1413: a multi-wavelengths analysis

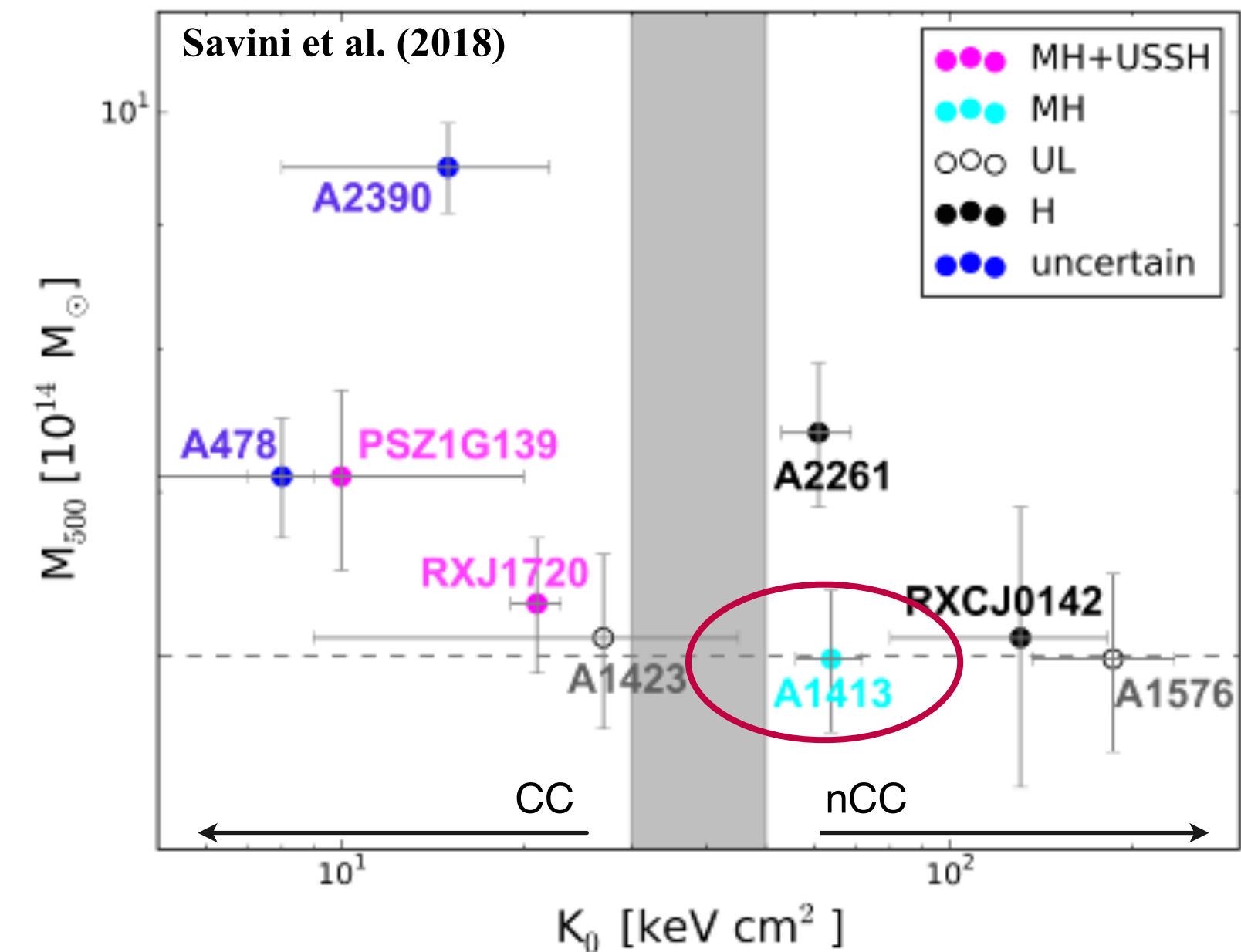


Savini et al. (2018)

Merging vs non merging merger

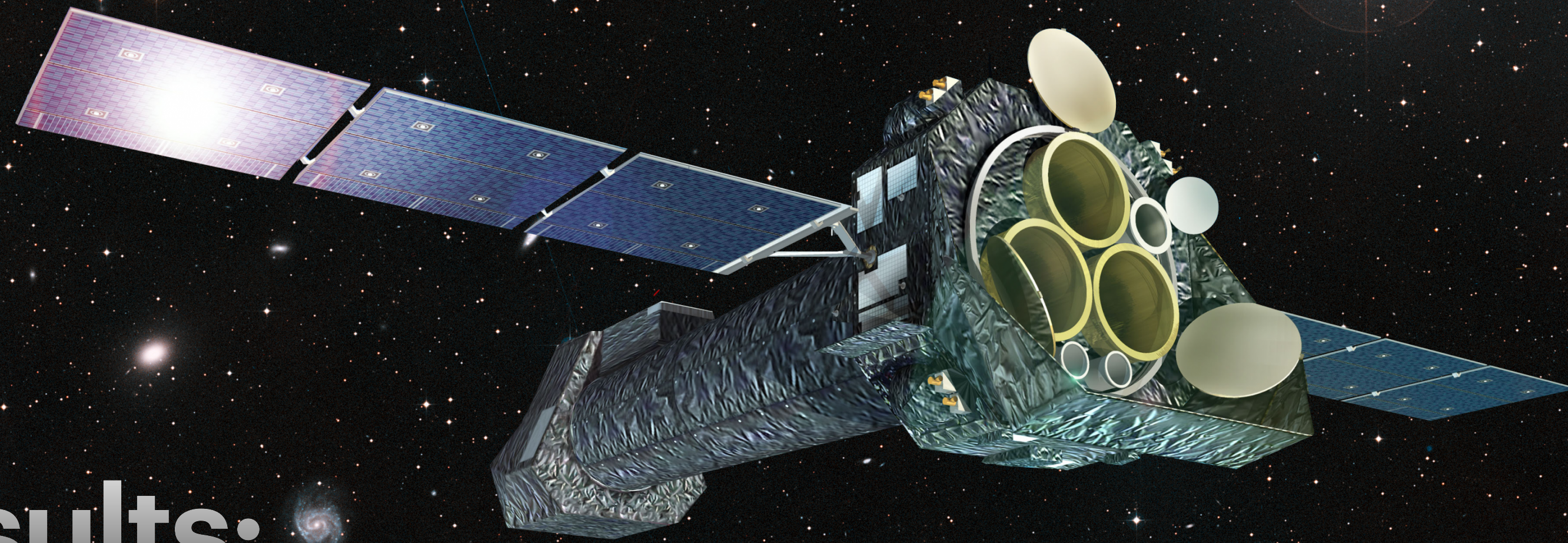


CoolCore vs non CoolCore



New updated multi-wavelengths analysis of A1413, by

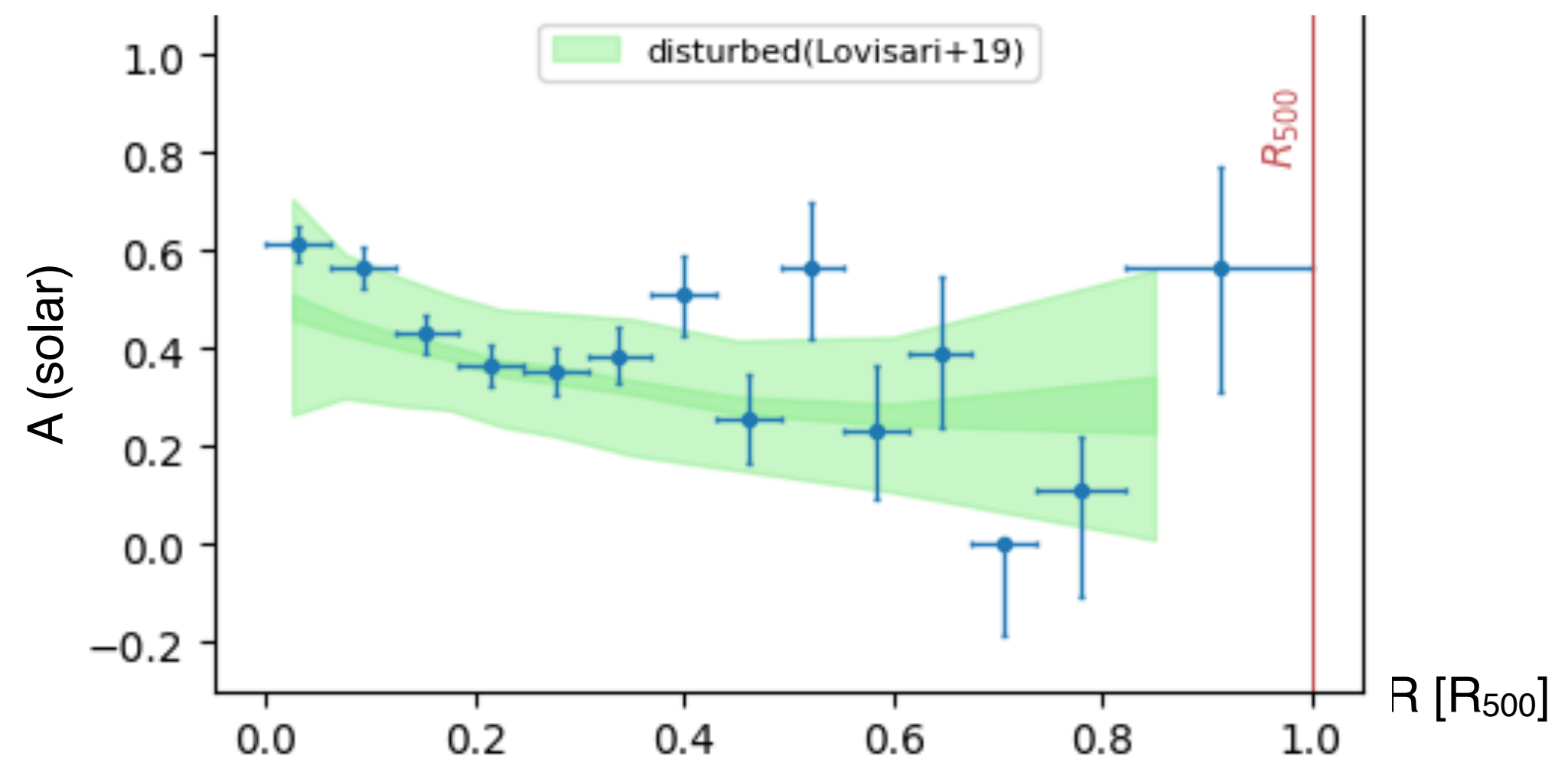
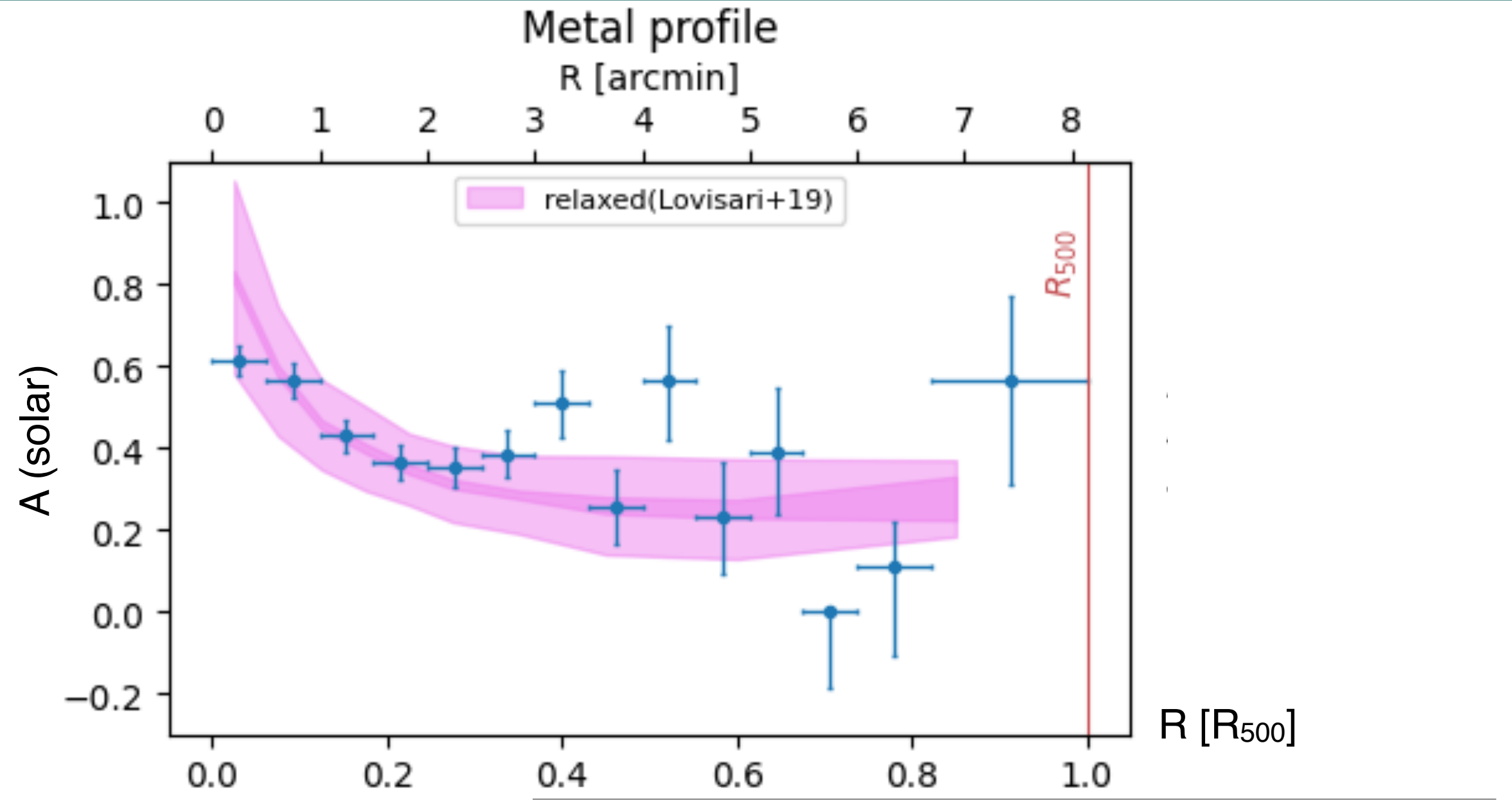
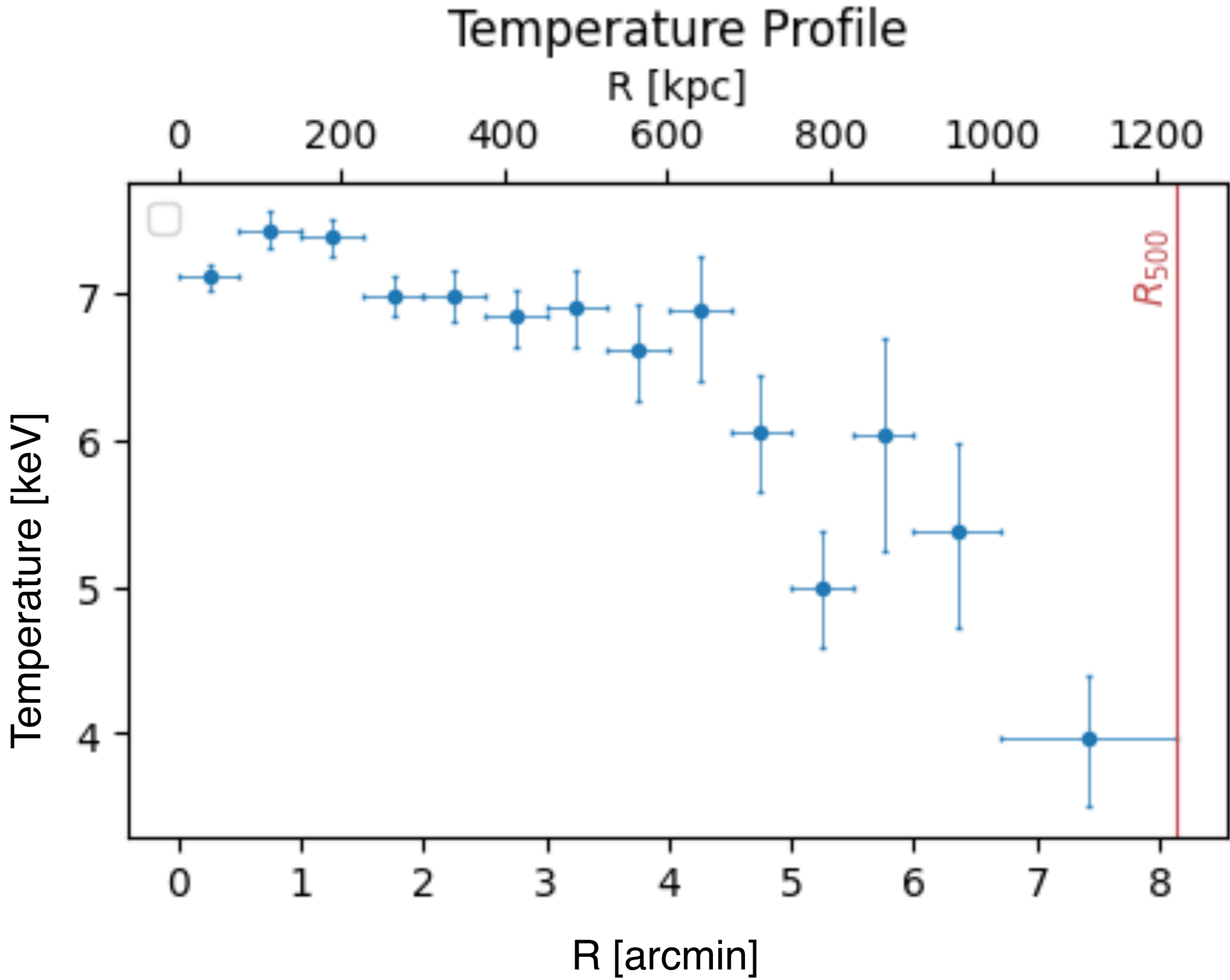
- characterizing the **dynamical state**, throughout the study of ICM properties
- determining the properties of the **diffuse radio emission** hosted by the cluster.



X-ray results:

Newly processed
XMM-Newton archive data of A1413
(~80 ks observation)

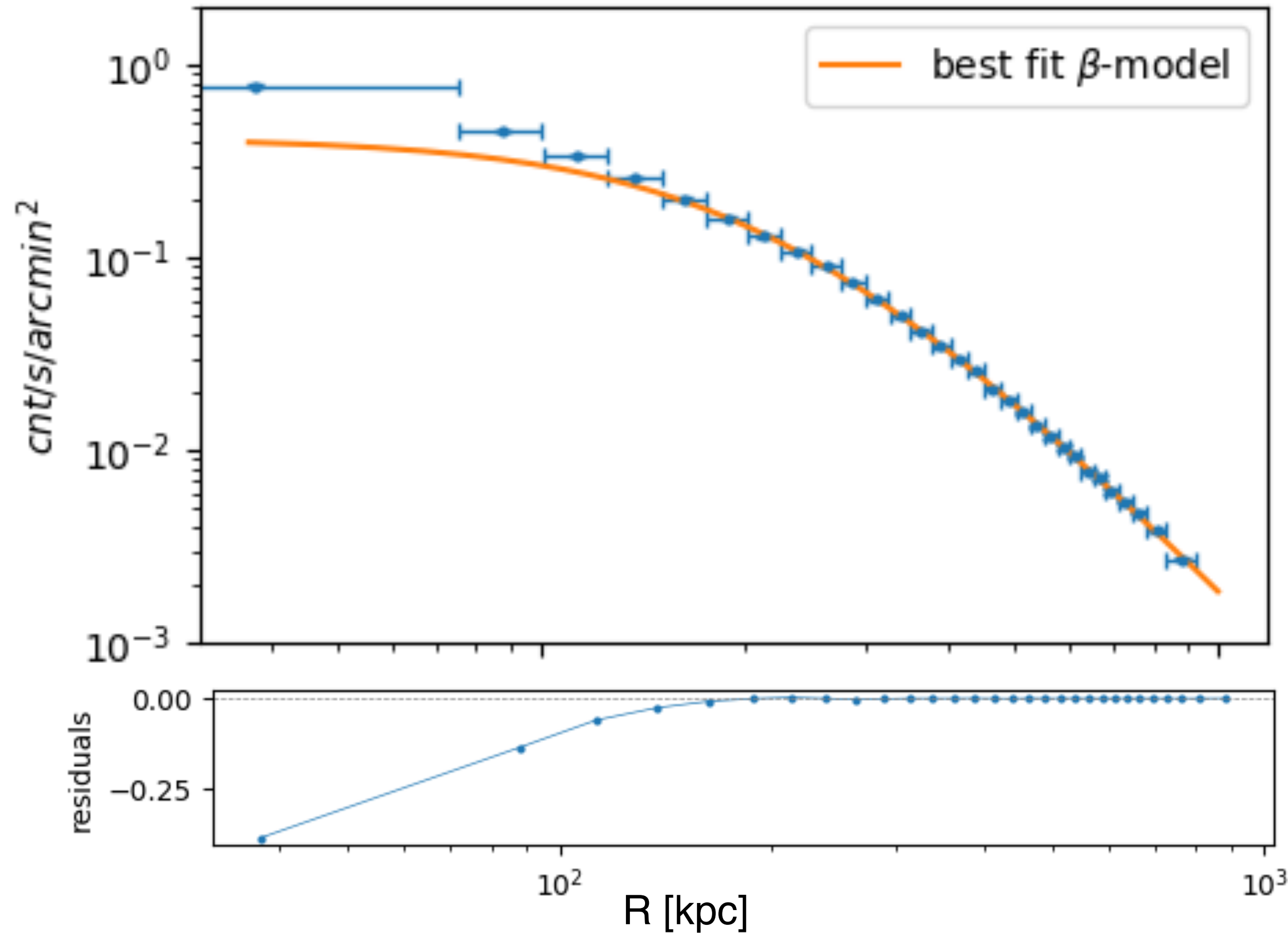
Spectral profiles



Surface brightness profile

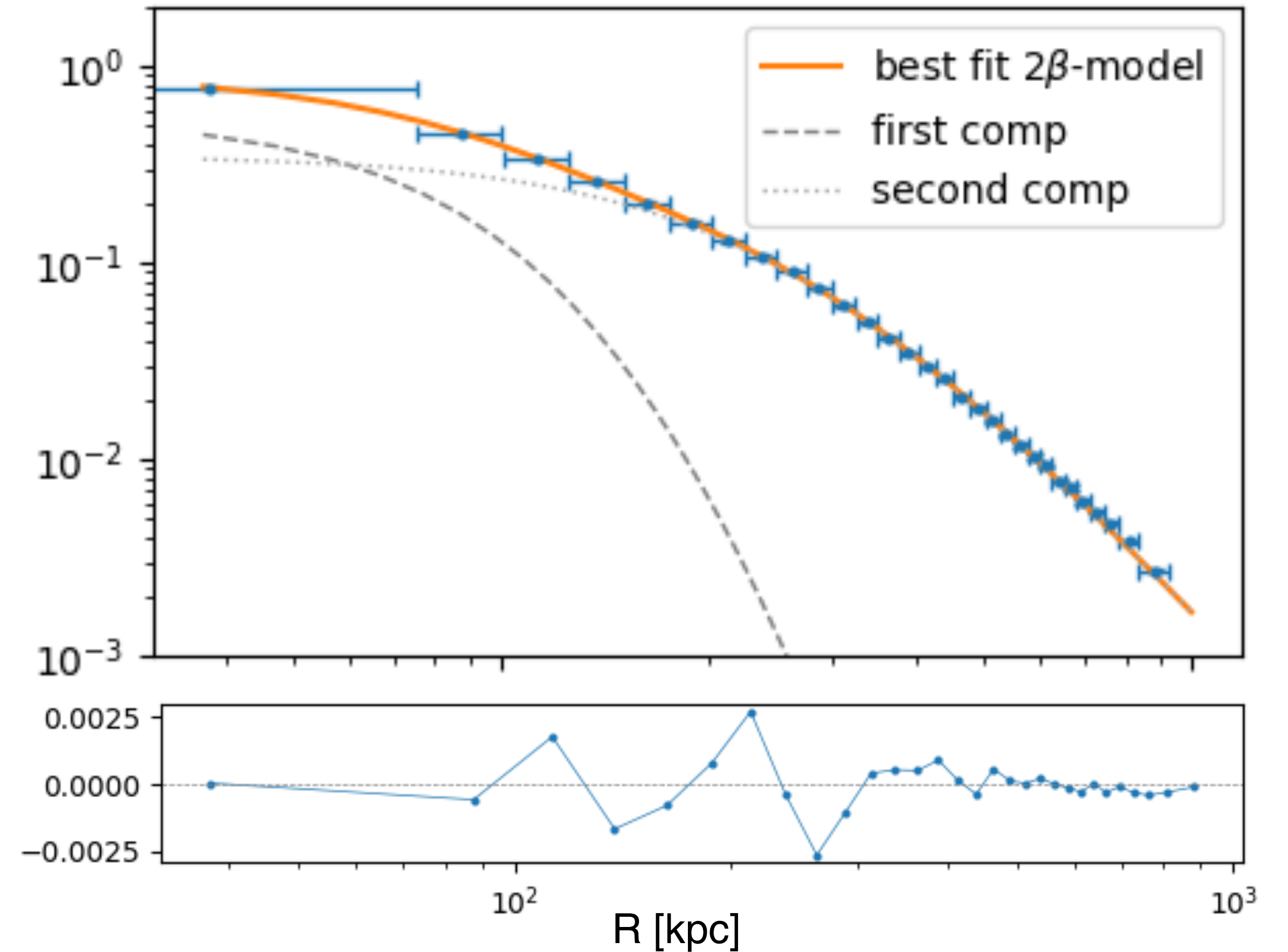
$$S(r) = S_0 \left[1 + \left(\frac{r}{r_c} \right) \right]^{-3\beta_1 + 0.5}$$

Surface brightness profile



$$S(r) = S_{0,1} \left[1 + \left(\frac{r}{r_{c,1}} \right) \right]^{-3\beta_1 + 0.5} + S_{0,2} \left[1 + \left(\frac{r}{r_{c,2}} \right) \right]^{-3\beta_2 + 0.5}$$

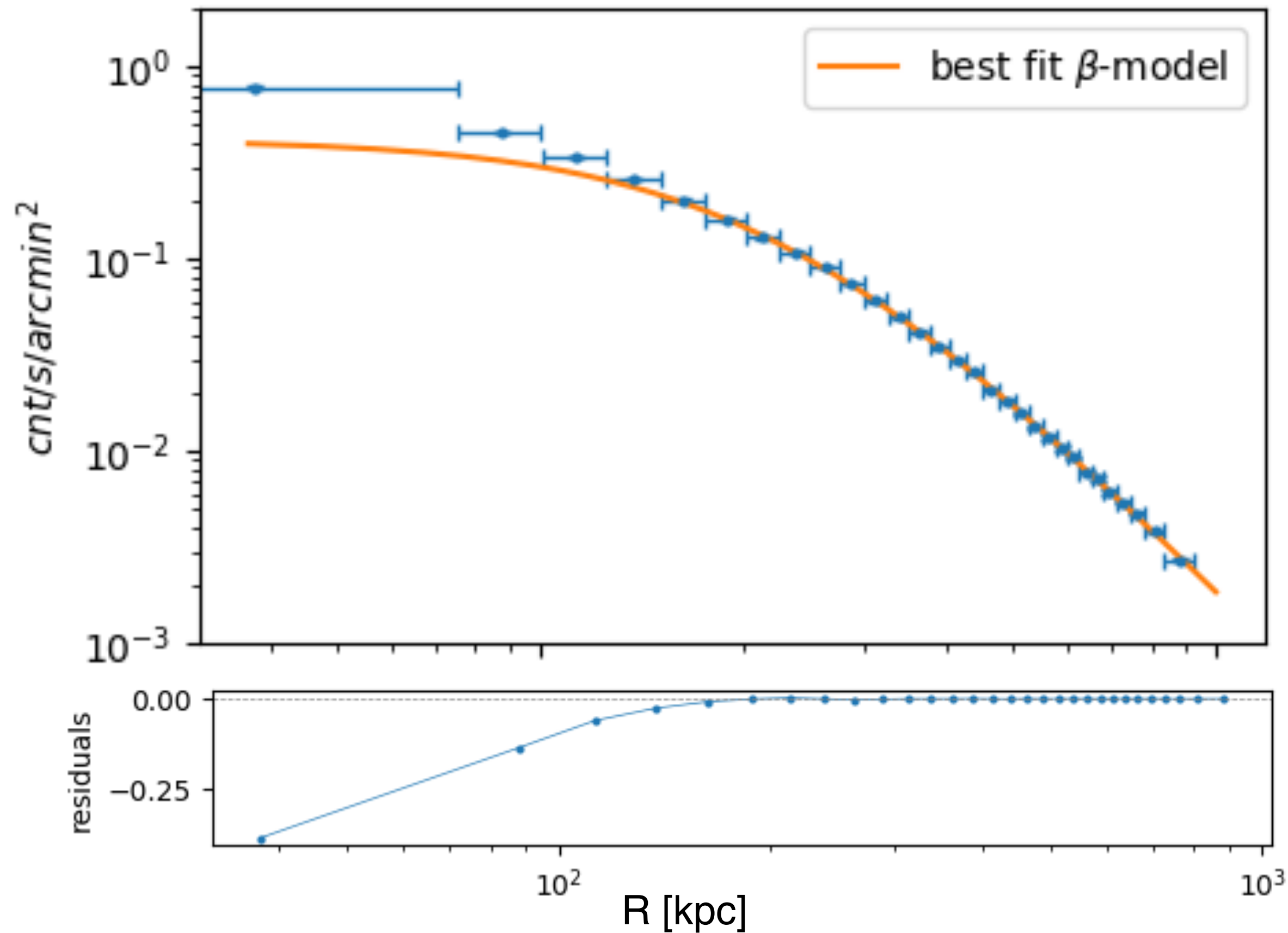
Surface brightness profile 2β -model



Surface brightness profile

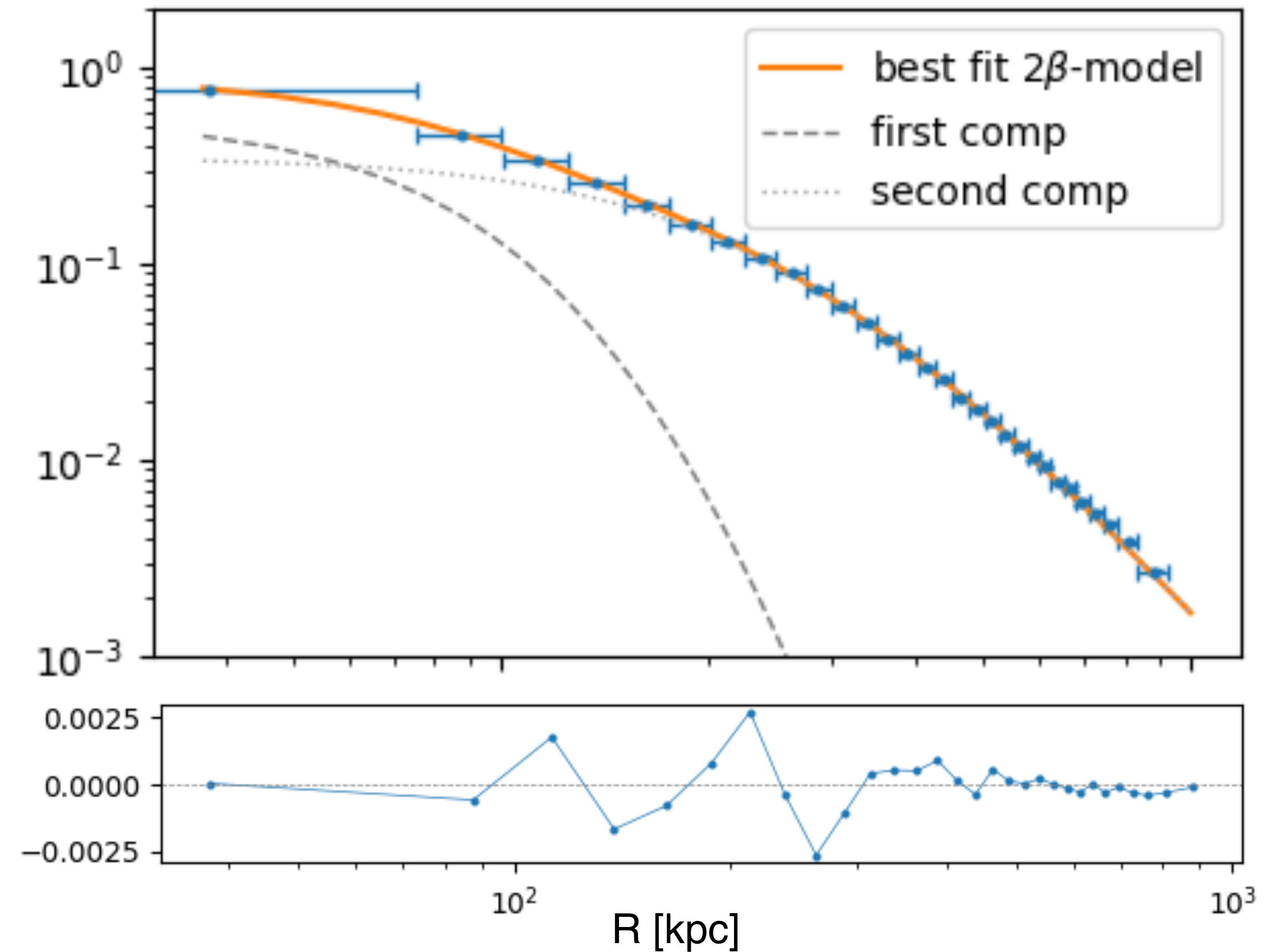
$$S(r) = S_0 \left[1 + \left(\frac{r}{r_c} \right) \right]^{-3\beta_1 + 0.5}$$

Surface brightness profile

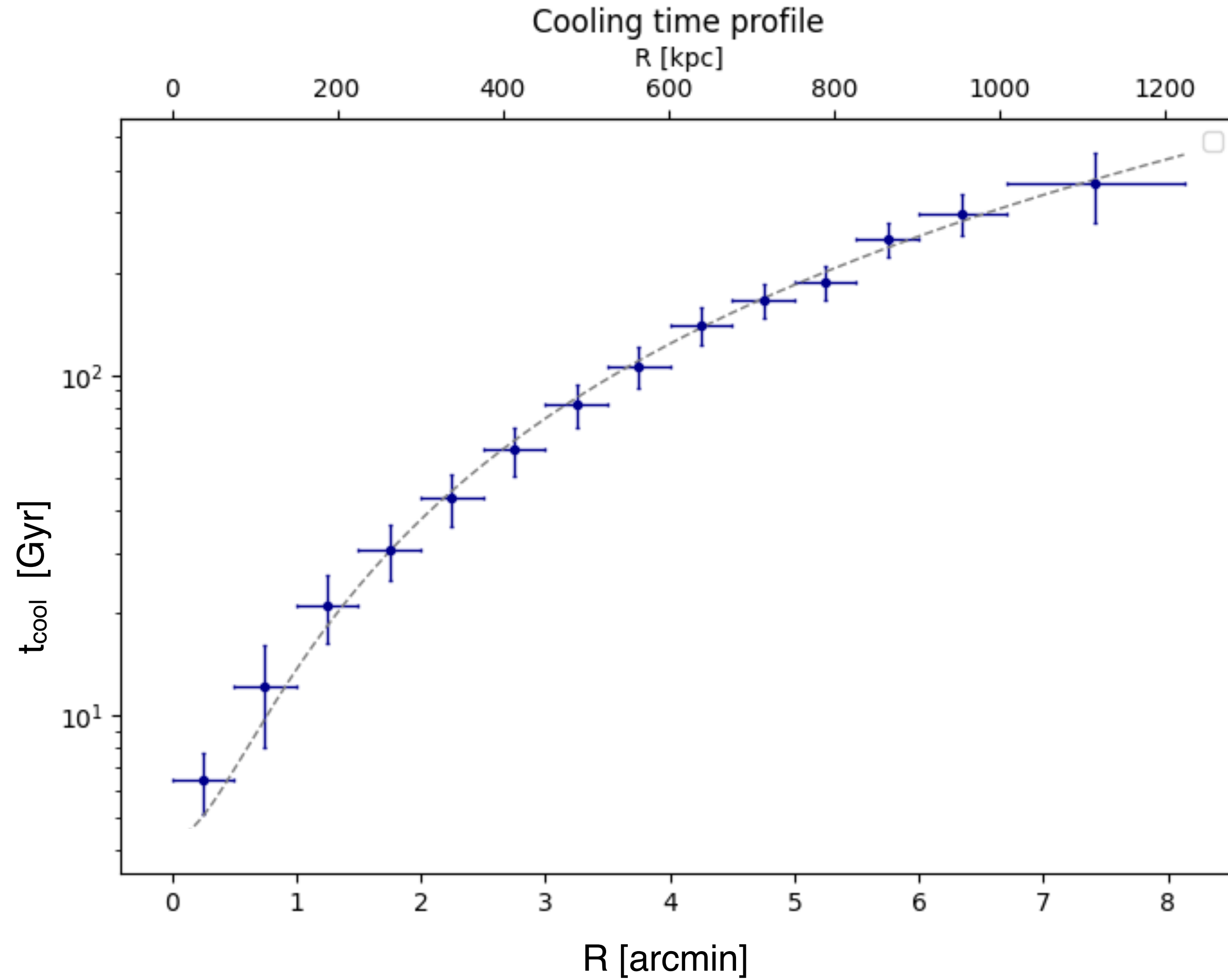


$$S(r) = S_{0,1} \left[1 + \left(\frac{r}{r_{c,1}} \right) \right]^{-3\beta_1 + 0.5} + S_{0,2} \left[1 + \left(\frac{r}{r_{c,2}} \right) \right]^{-3\beta_2 + 0.5}$$

Surface brightness profile 2β -model

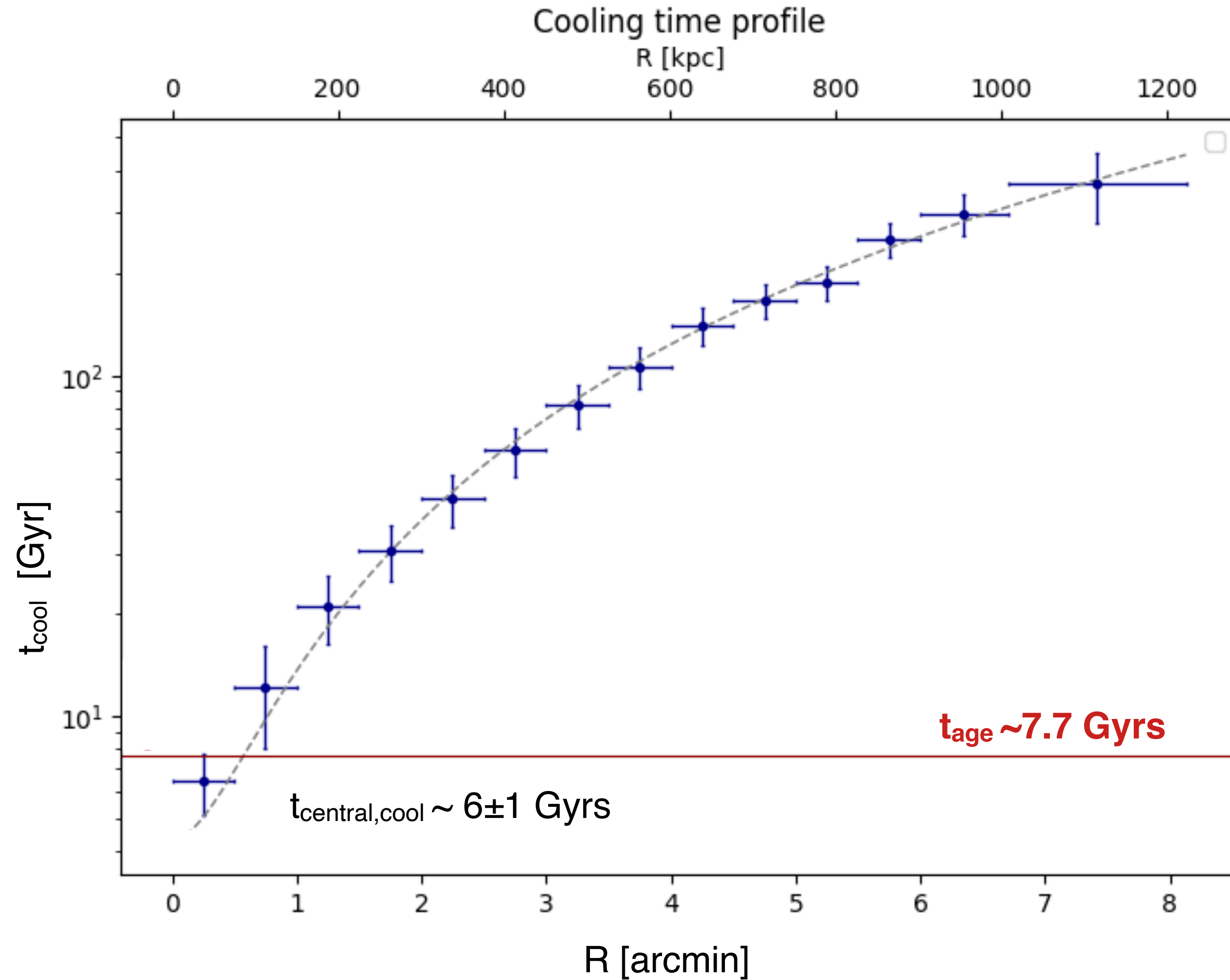


Cooling time profile



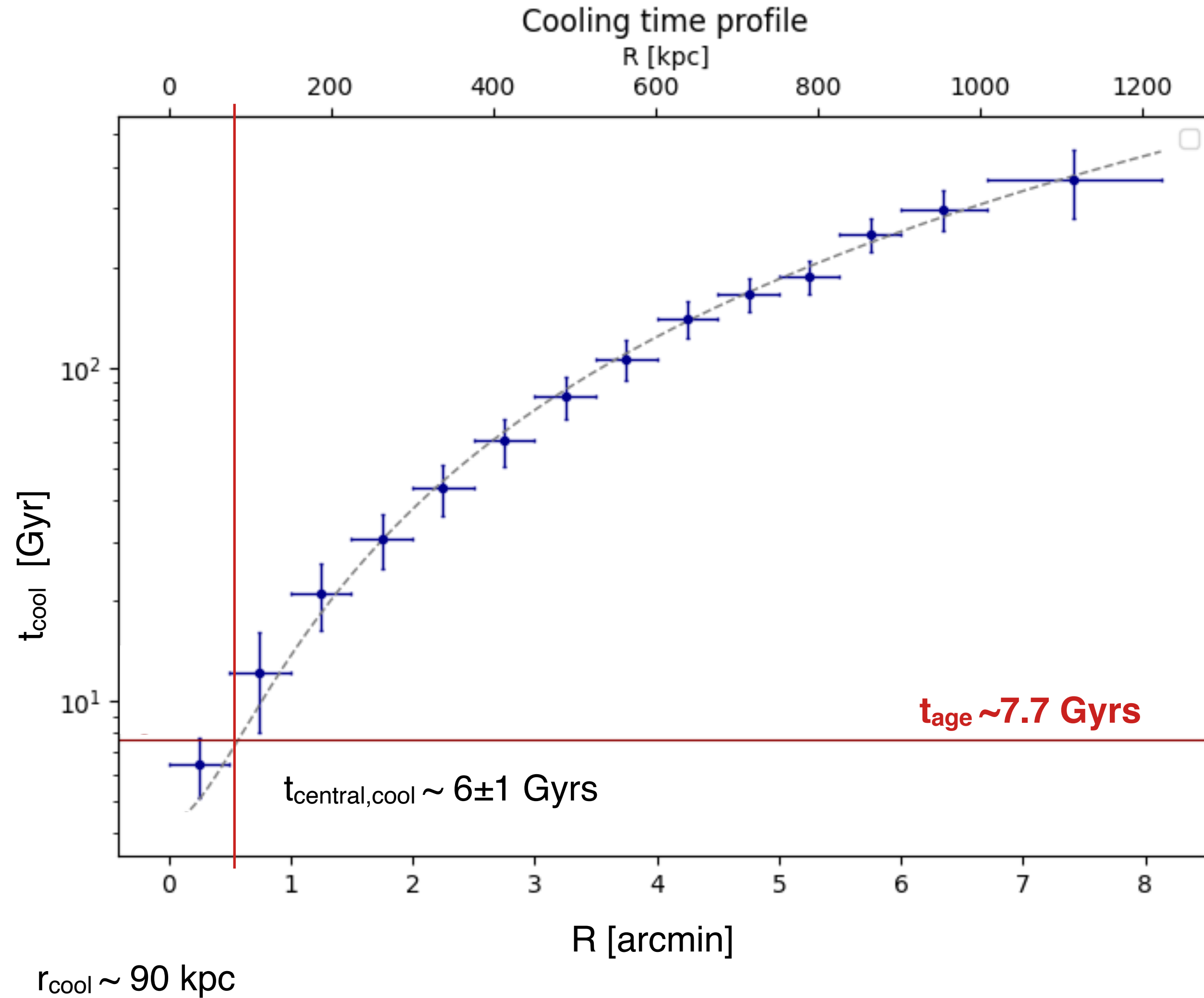
$$t_{cool} = \frac{H}{\Lambda(T)n_en_p} = \frac{\gamma}{\gamma - 1} \frac{kT(r)}{\mu X n_e(r) \Lambda(T)}$$

Cooling time profile



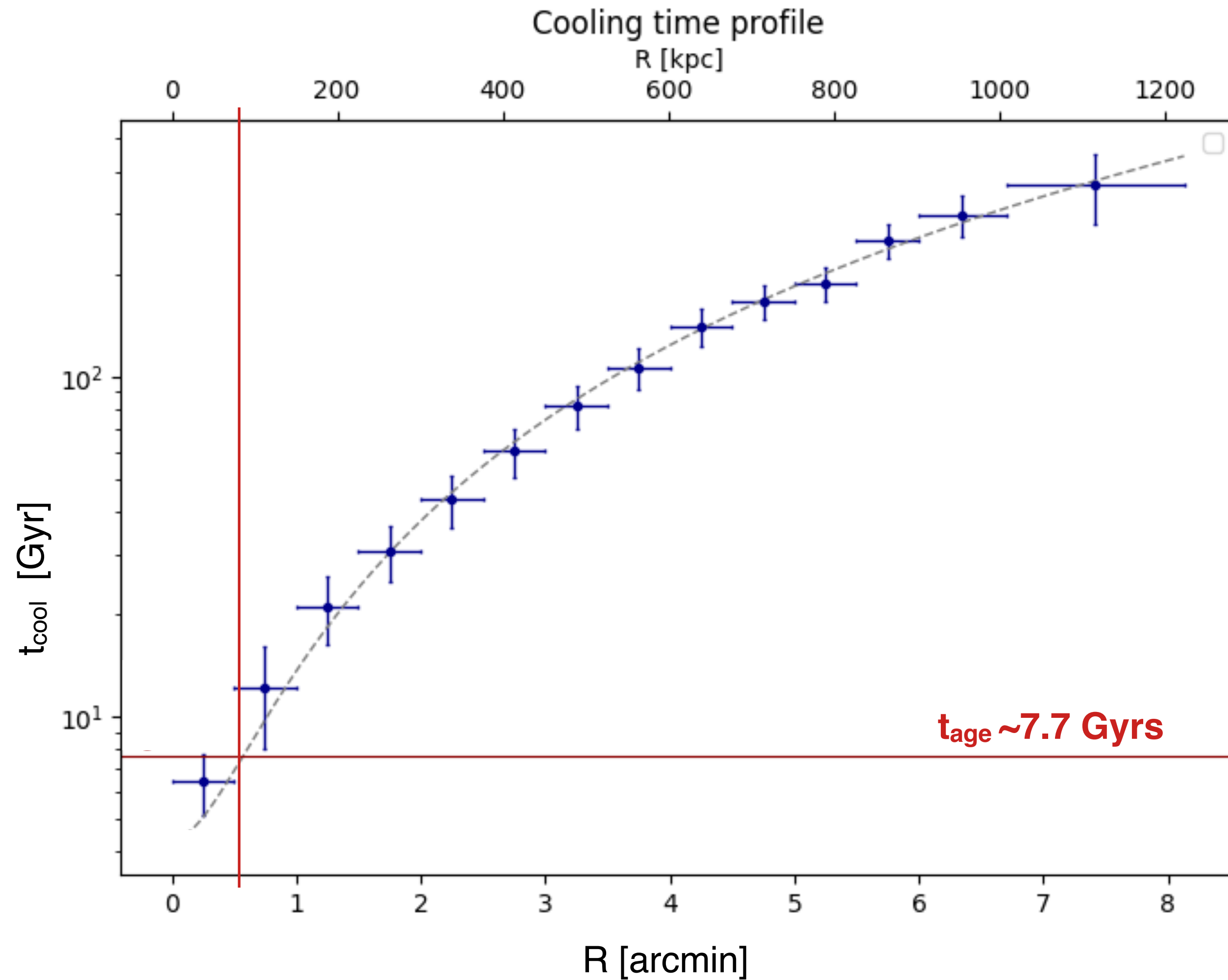
$$t_{cool} = \frac{H}{\Lambda(T)n_e n_p} = \frac{\gamma}{\gamma - 1} \frac{kT(r)}{\mu X n_e(r) \Lambda(T)}$$

Cooling time profile



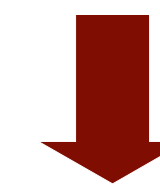
$$t_{cool} = \frac{H}{\Lambda(T)n_en_p} = \frac{\gamma}{\gamma - 1} \frac{kT(r)}{\mu X n_e(r) \Lambda(T)}$$

Cooling time profile



$$t_{cool} = \frac{H}{\Lambda(T)n_e n_p} = \frac{\gamma}{\gamma - 1} \frac{kT(r)}{\mu X n_e(r) \Lambda(T)}$$

$t_{central,cool} \sim 6 \pm 1$ Gyrs
 $r_{cool} \sim 90$ kpc



weak-cool-core system

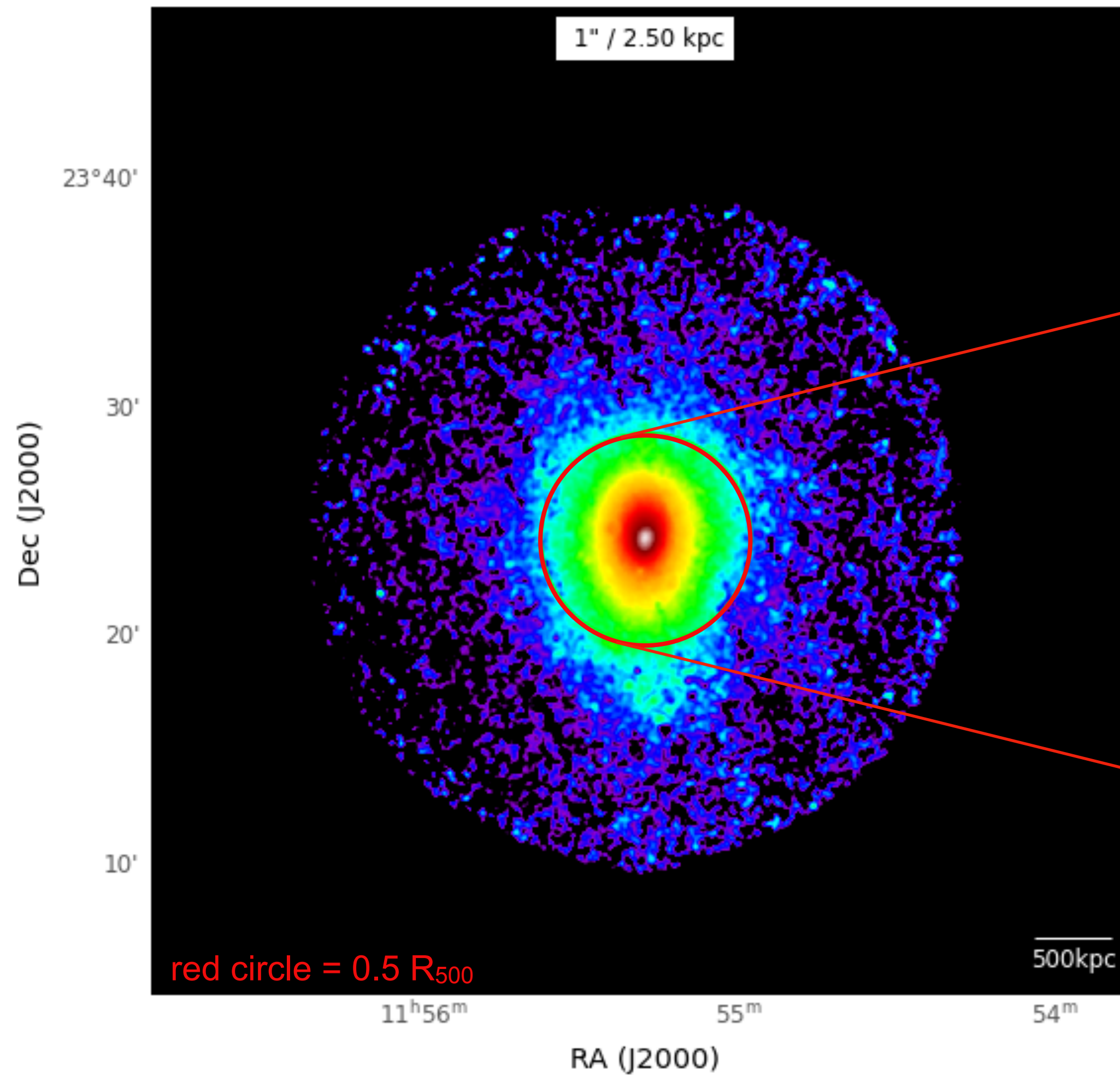
$1 \text{ Gyr} < t_{central,cool} < 7.7 \text{ Gyr} \sim t_{age}$

VS

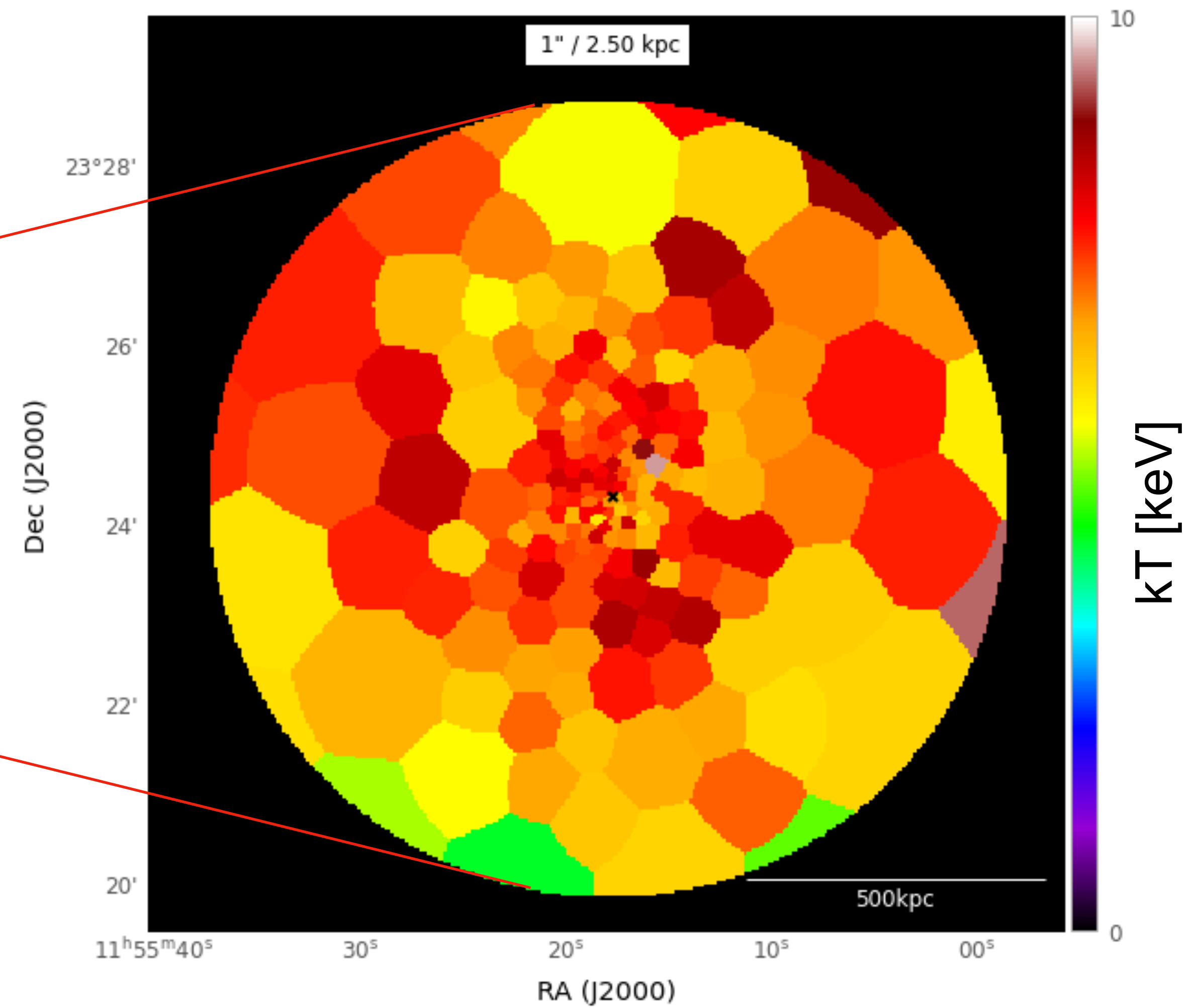
strong cool-core clusters

$t_{central,cool} < 1 \text{ Gyr}$

2D temperature map



Background-subtracted and exposure-corrected image of A1413 in [0.3,7] keV



Temperature map *within* 0.5 R_{500}

X-ray summary

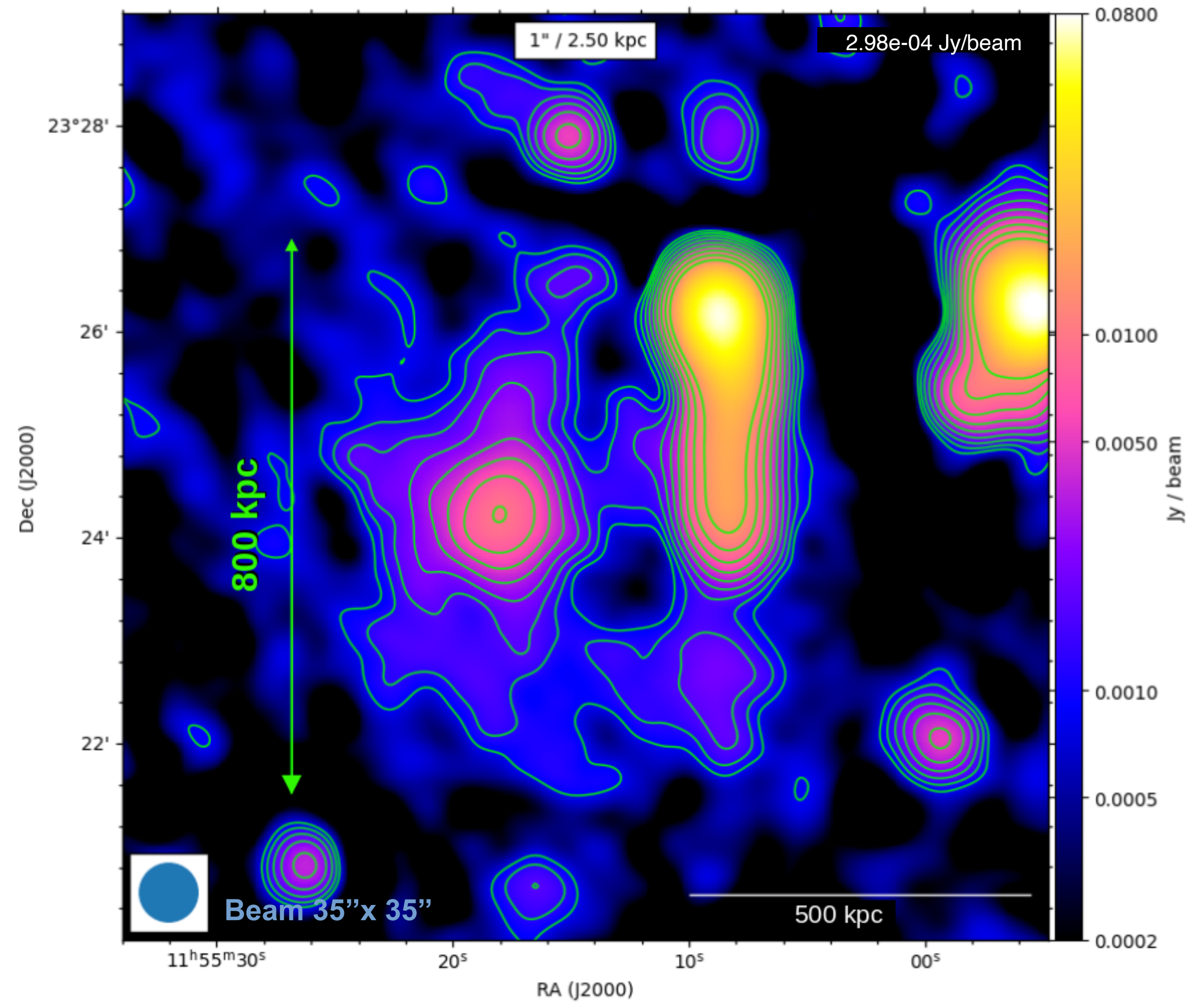
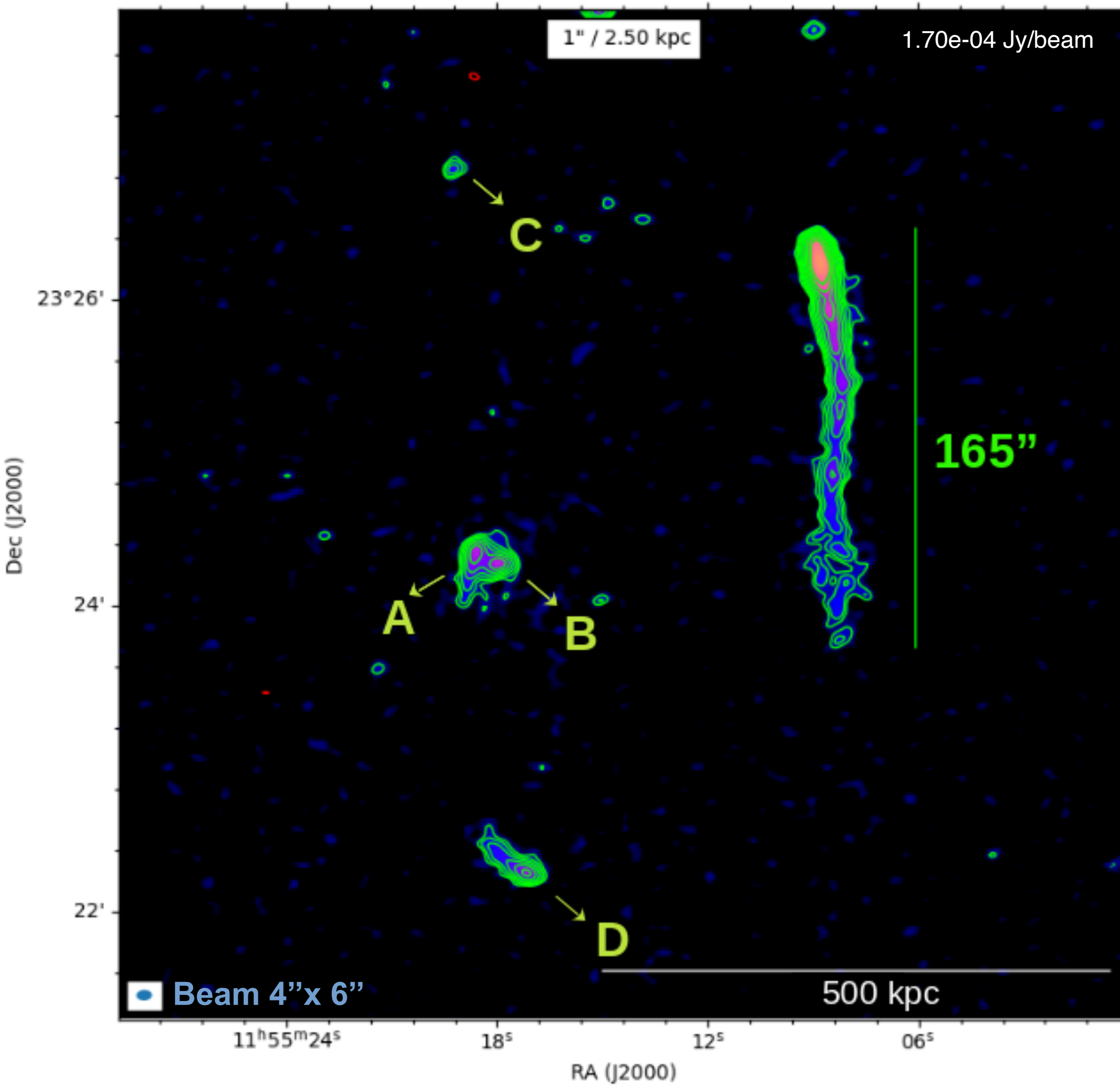
- Peculiar dynamical status of A1413
- A1413 has no disrupted morphology, but the elliptical shape of the surface brightness, the kT & Z azimuthal profiles, the cooling time and the variation of the 2D temperature map, suggest that it could have experienced a past of (minor) merger events → **not fully relaxed systems**
- A1413 has $t_{central,cool} \sim 6 \text{ Gyr} < 7.7 \text{ Gyr} \sim t_{age}$ → **weak-cool-core systems**

Radio results:

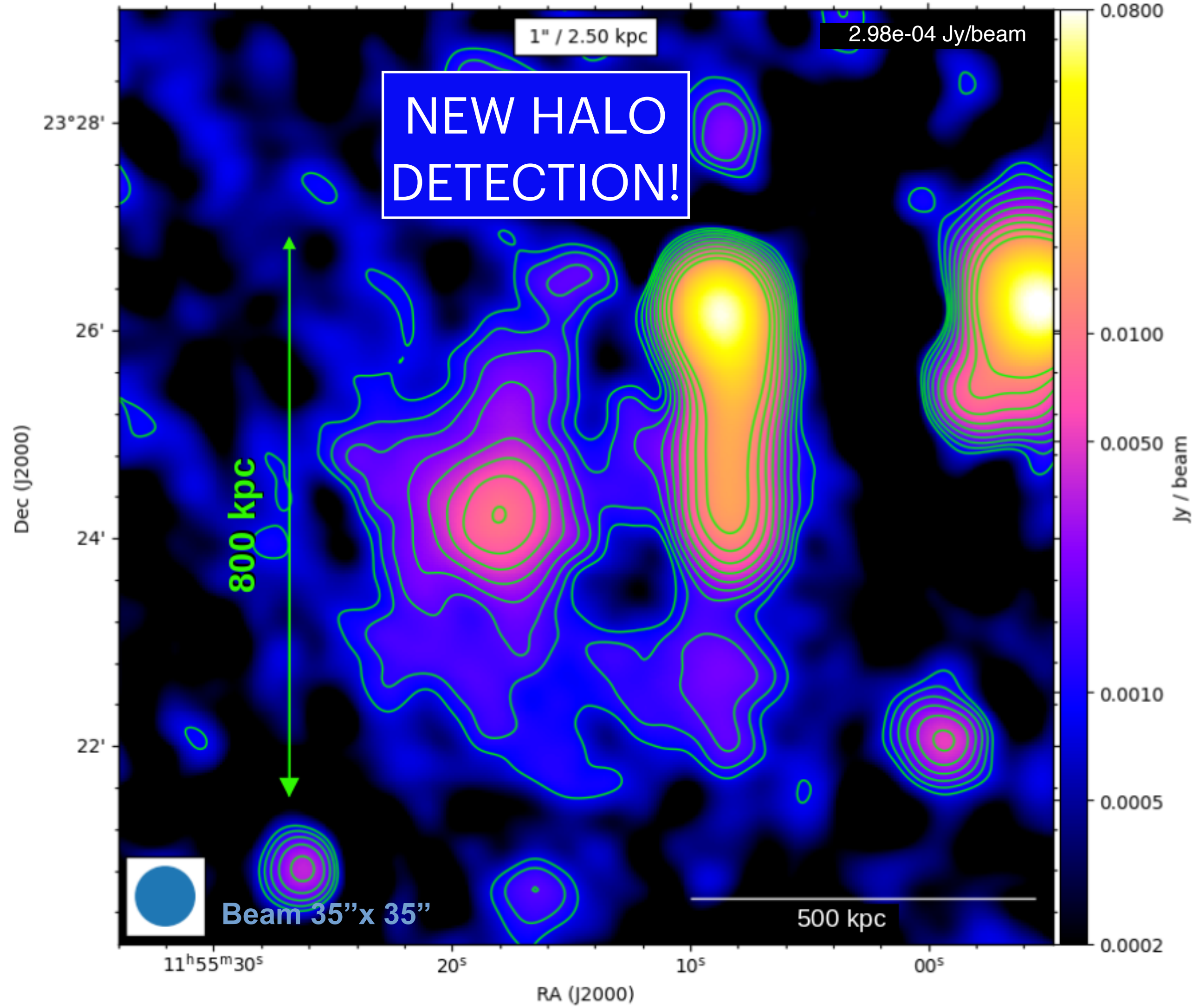
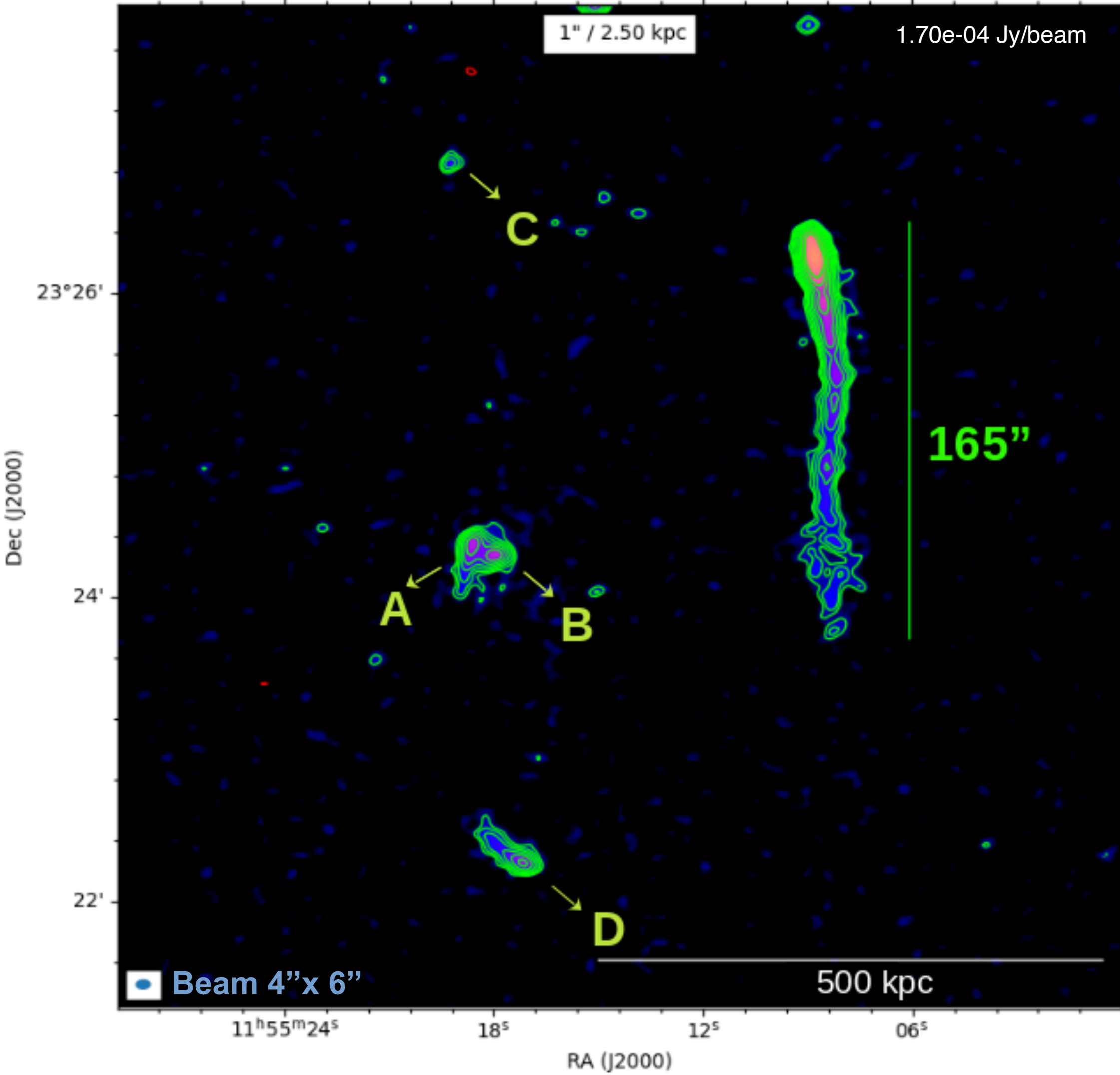
Imaging of new **LOFAR** observation
from the LoTTS survey @144 MHz



Imaging at low and high resolution

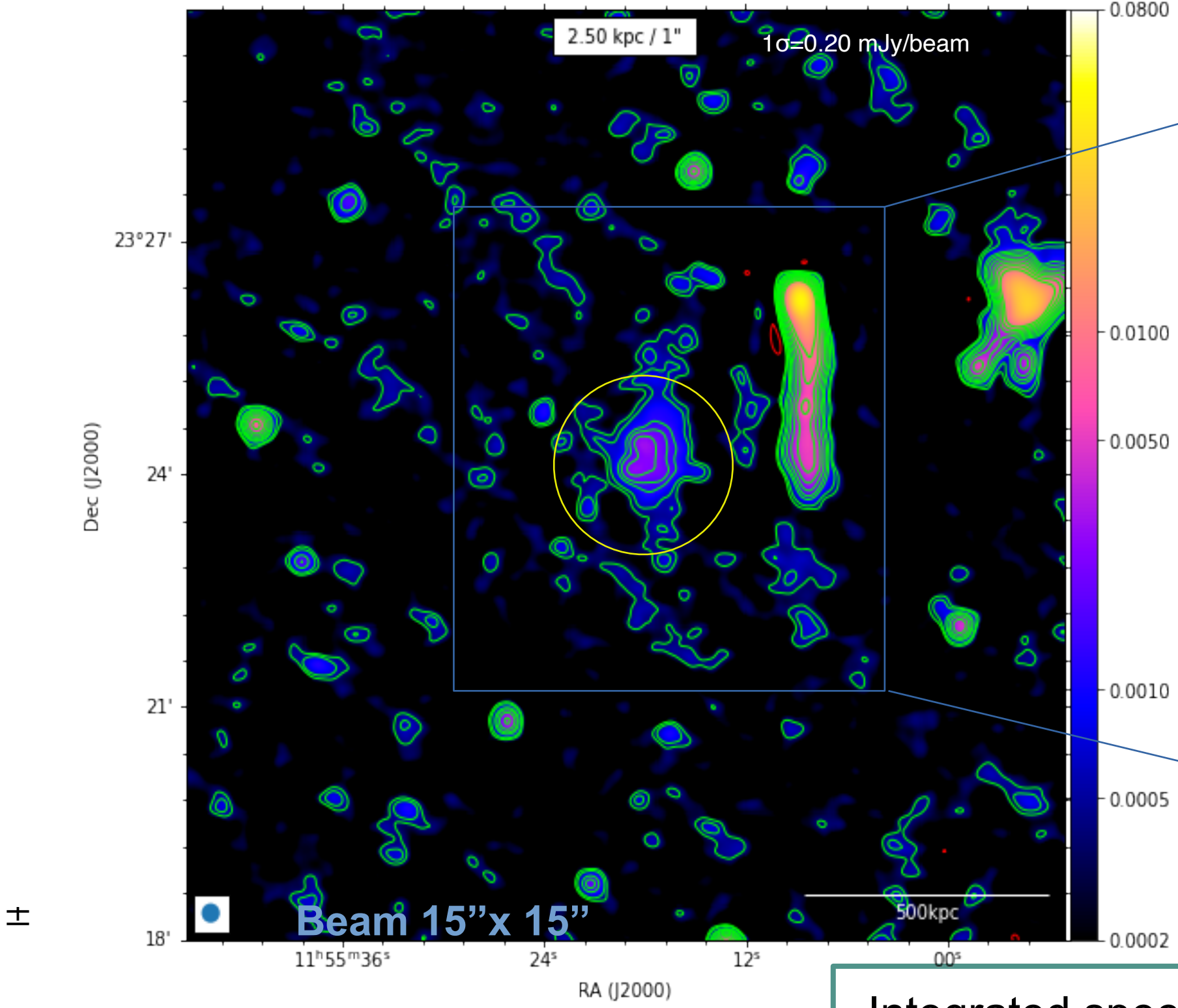


Imaging at low and high resolution

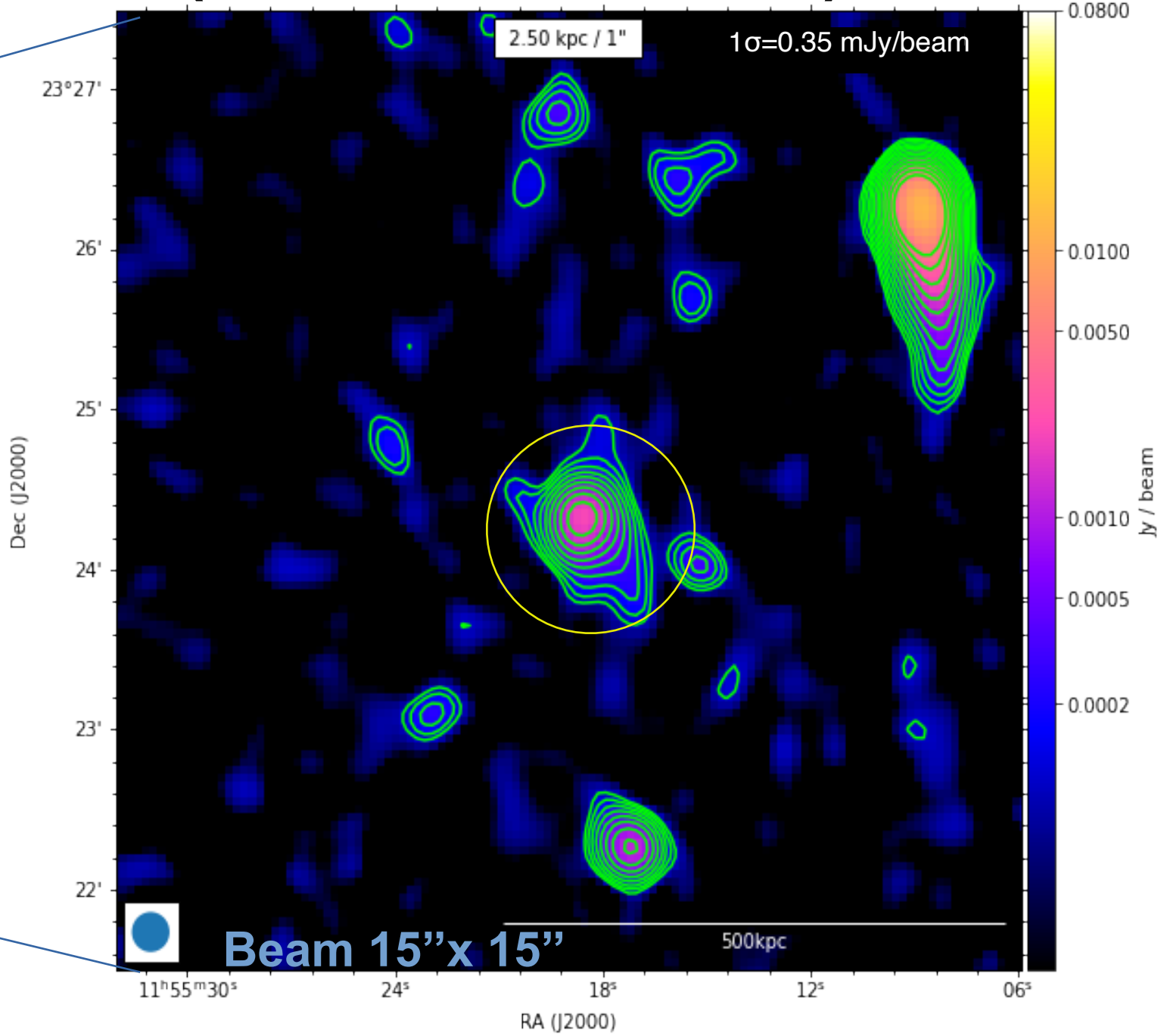


Comparison with high frequency data

LOFAR 114MHz image



VLA 1.4GHz image (Govoni et al. 2009)

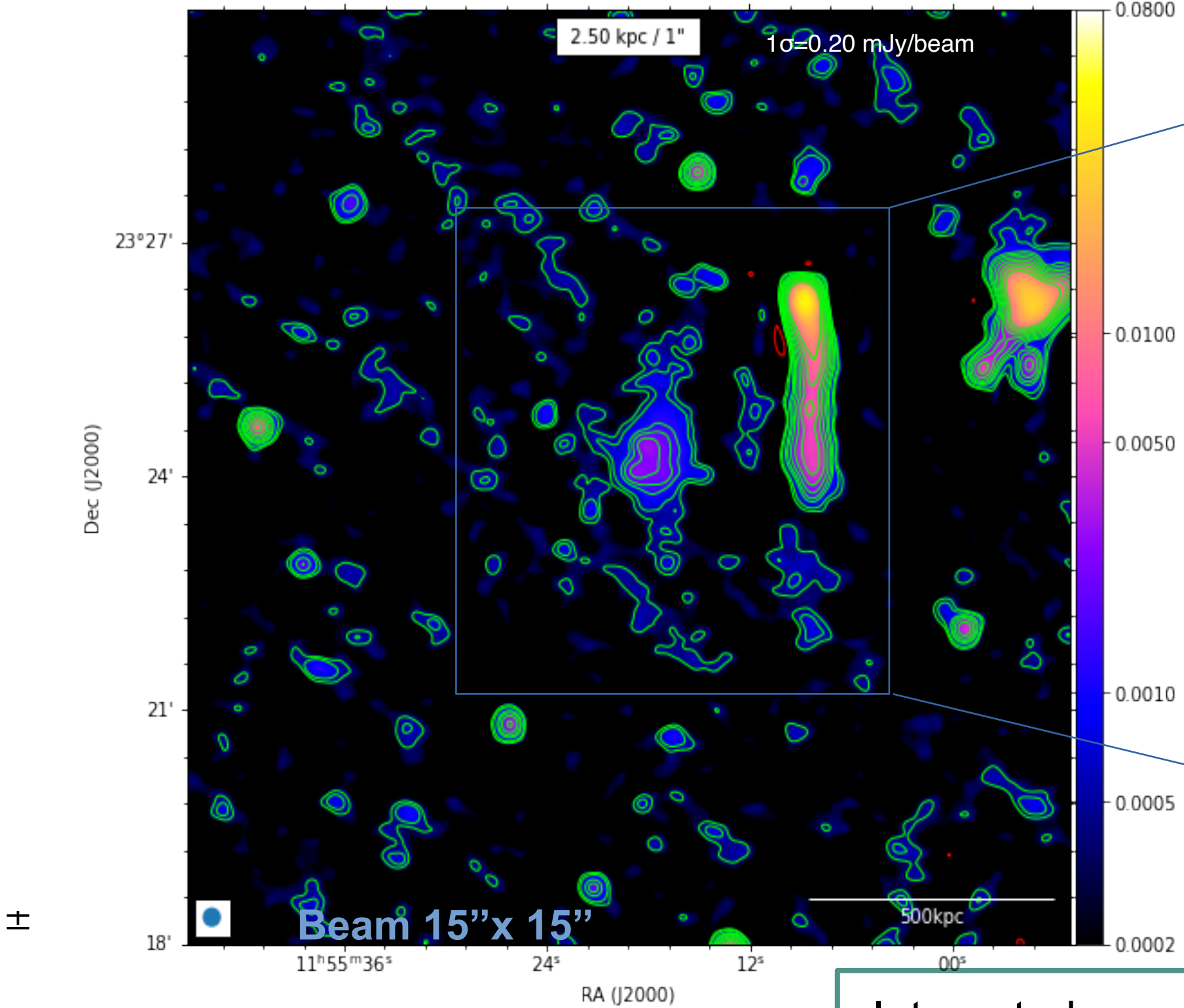


Integrated spectral index of central region
 $S_{\nu} \sim \nu^{-\alpha}$
 $\alpha = 1.1 \pm 0.2$

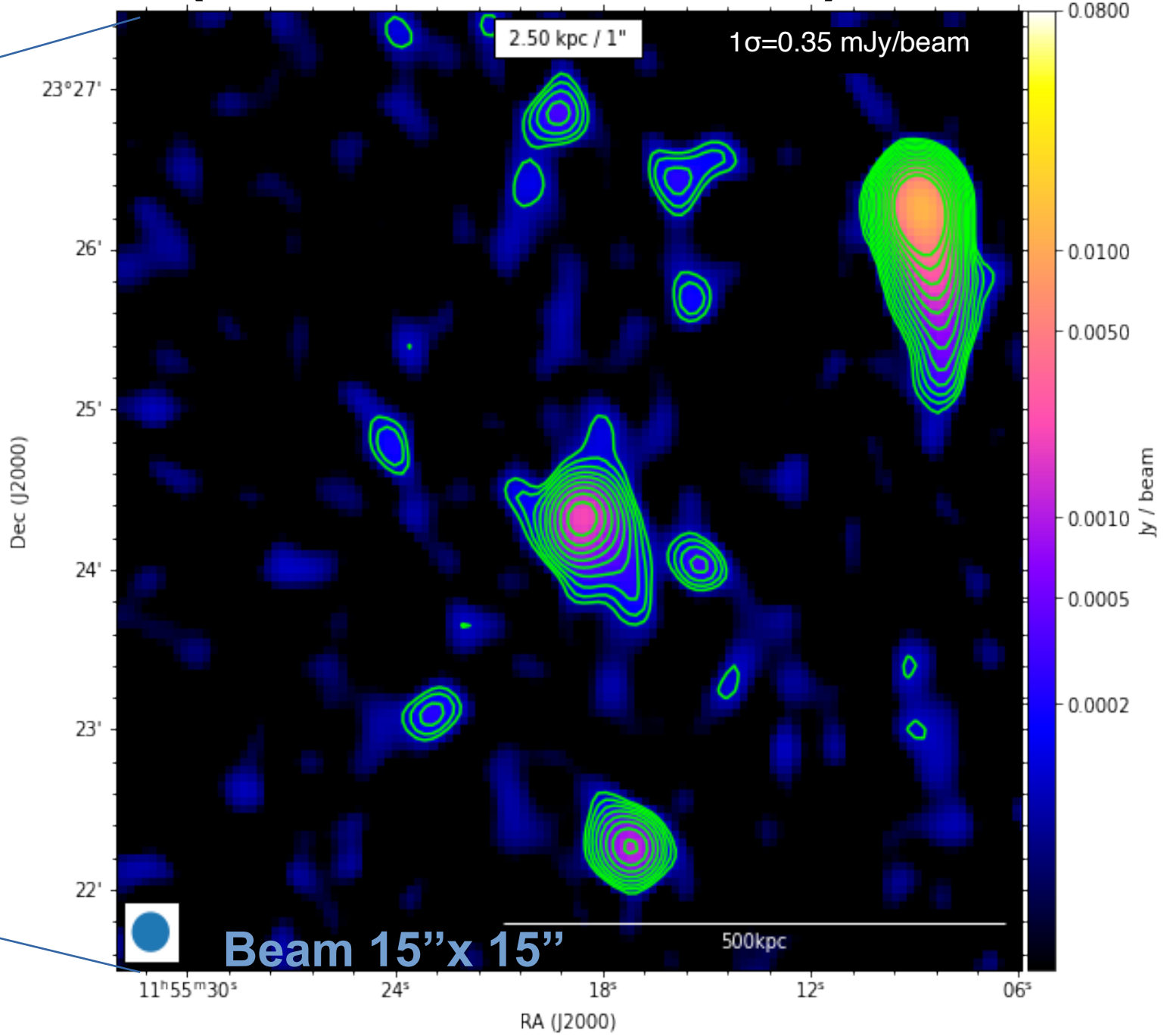
→ typical of mini-halo

Comparison with high frequency data

LOFAR 114MHz image



VLA 1.4GHz image
(Govoni et al. 2009)



Integrated spectral index of central region
 $S_{\nu} \sim \nu^{-\alpha}$
 $\alpha = 1.1 \pm 0.2$
 1 σ limit for the **extended** emission
 $\alpha > 1.6$

→ typical of mini-halo

Halo emission analysis

Radio Power – X-ray Luminosity relation

$$P_{1.4\text{GHz}} \propto L_{\text{X-ray}}$$

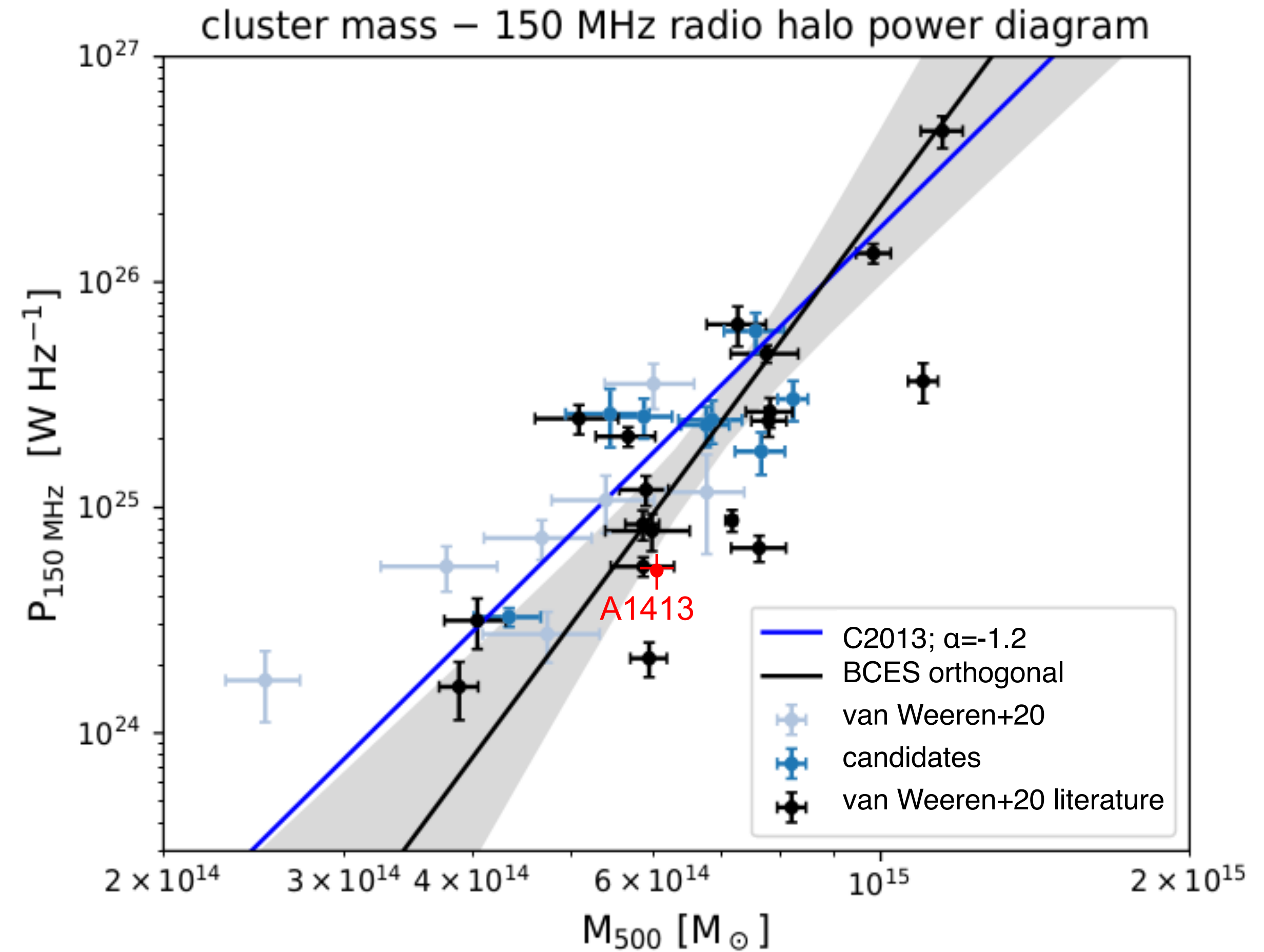


Radio Power – Mass relation

$$P_{144\text{MHz}} \propto M_{500}$$

$$P_{\text{halo}} = 5.2 \pm 0.6 \cdot 10^{24} \text{ W/Hz}$$

$$M_{500} = 5.9 \pm 0.2 \cdot 10^{14} M_{\text{sun}}$$



van Weeren et. al. 2020

Radio summary

- **New halo detection** in A1413 on ~800 kpc scale (N-S direction)
- A1413 hosts a **hybrid halo + mini-halo-like** radio source
- The 2 emissions have **different spectral index**

Point-to-point correlation

Point-to-point comparison between *radio* and *X-ray surface brightness*

$$\log(I_R) = A \log(I_X) + B$$

$A < 1$
radio brightness declines
slower
than X-ray

$A > 1$
radio brightness declines
faster
than X-ray

Point-to-point correlation

Point-to-point comparison between *radio* and *X-ray surface brightness*

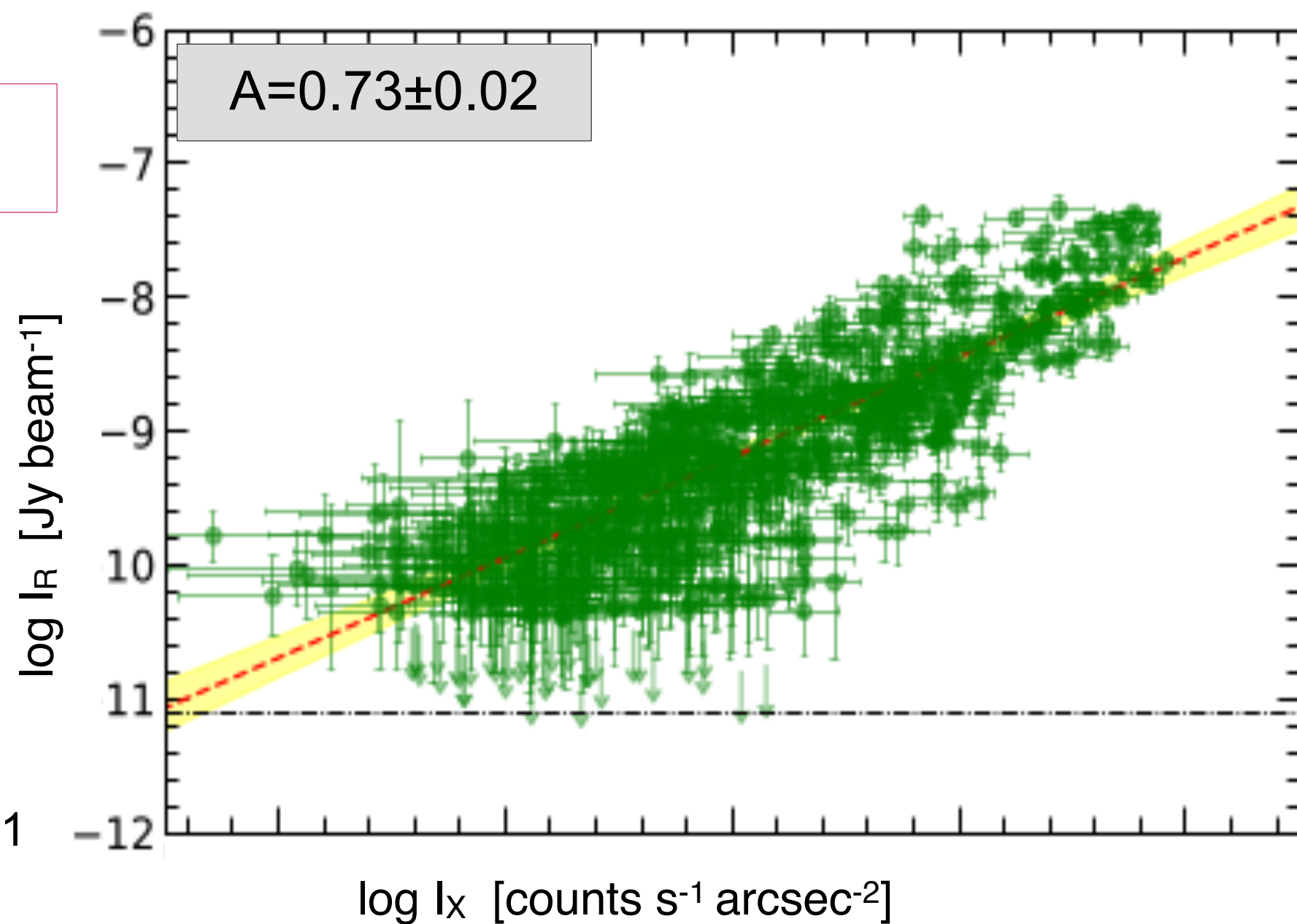
$$\log(I_R) = A \log(I_X) + B$$

$A < 1$
radio brightness declines
slower
than X-ray

$A > 1$
radio brightness declines
faster
than X-ray

HALOS

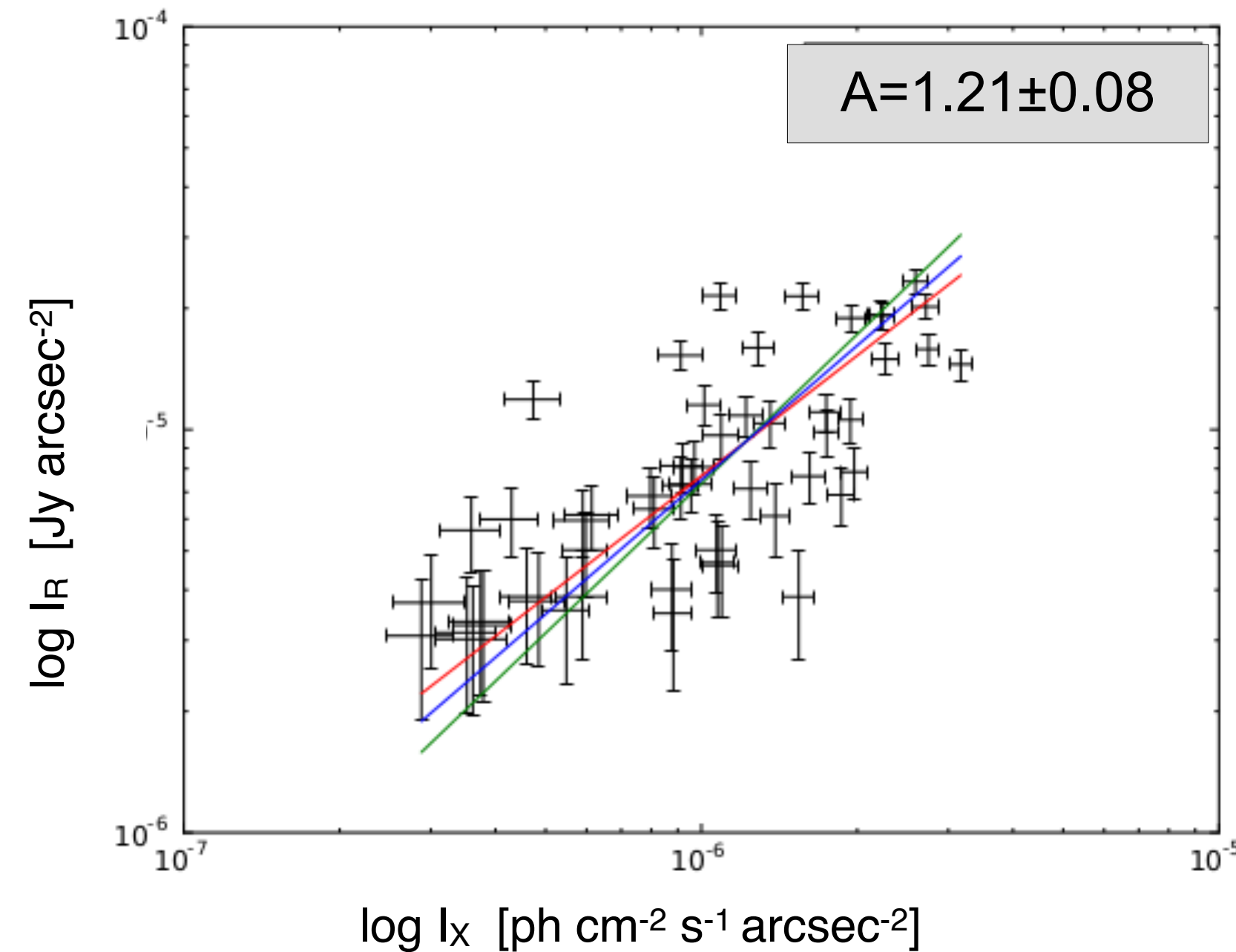
Linear
or
Sub-linear
scaling



Rajpurohit et al. 2021

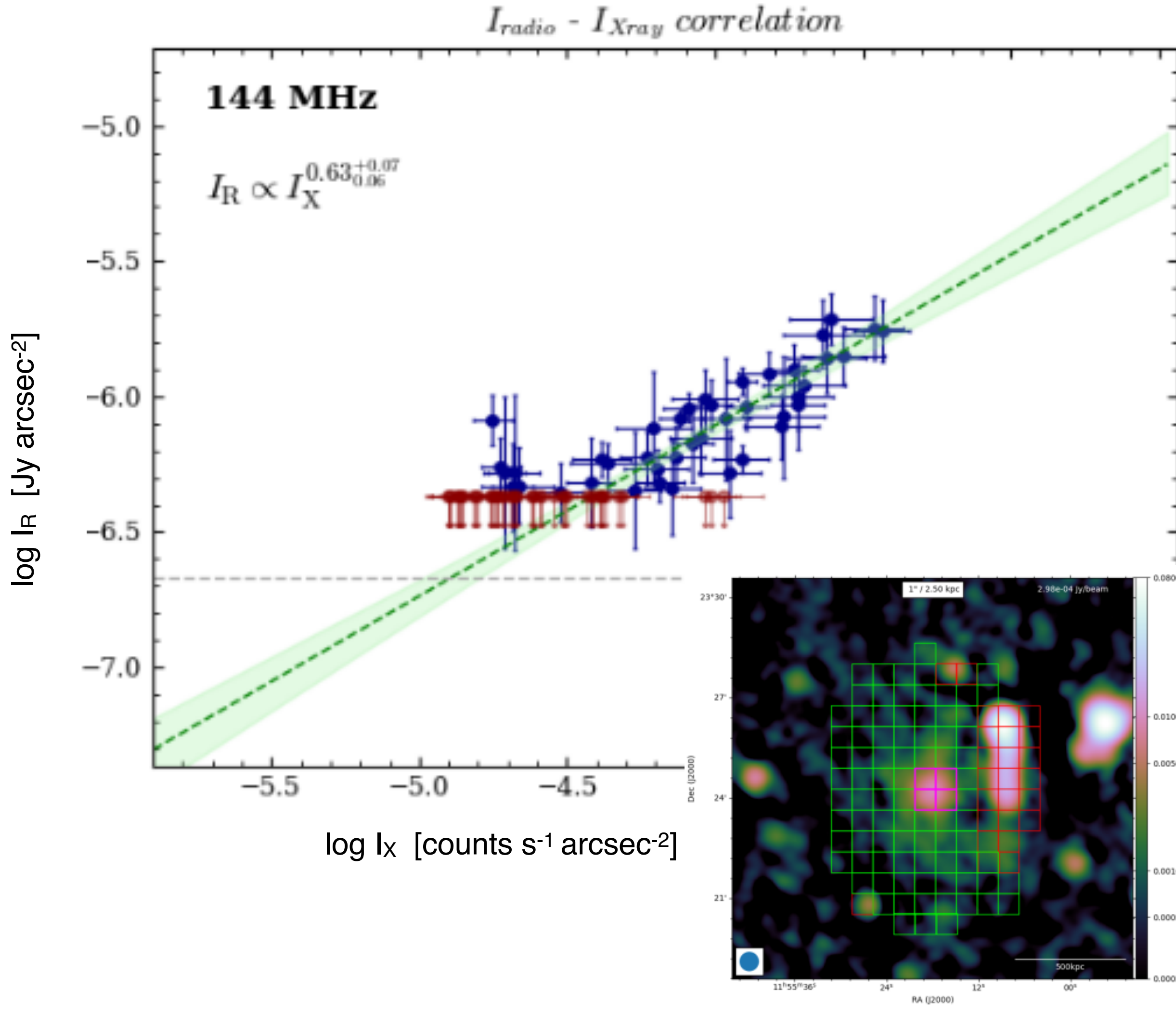
MINI-HALOS

Super-linear
scaling

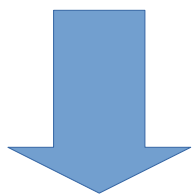


Ignesti et al. 2020

Point-to-point correlation: *halo emission*



Halo	Grid	A	r_p
$I_R - I_X$	35'' × 35''	0.63 ^{0.07} _{0.06}	0.82



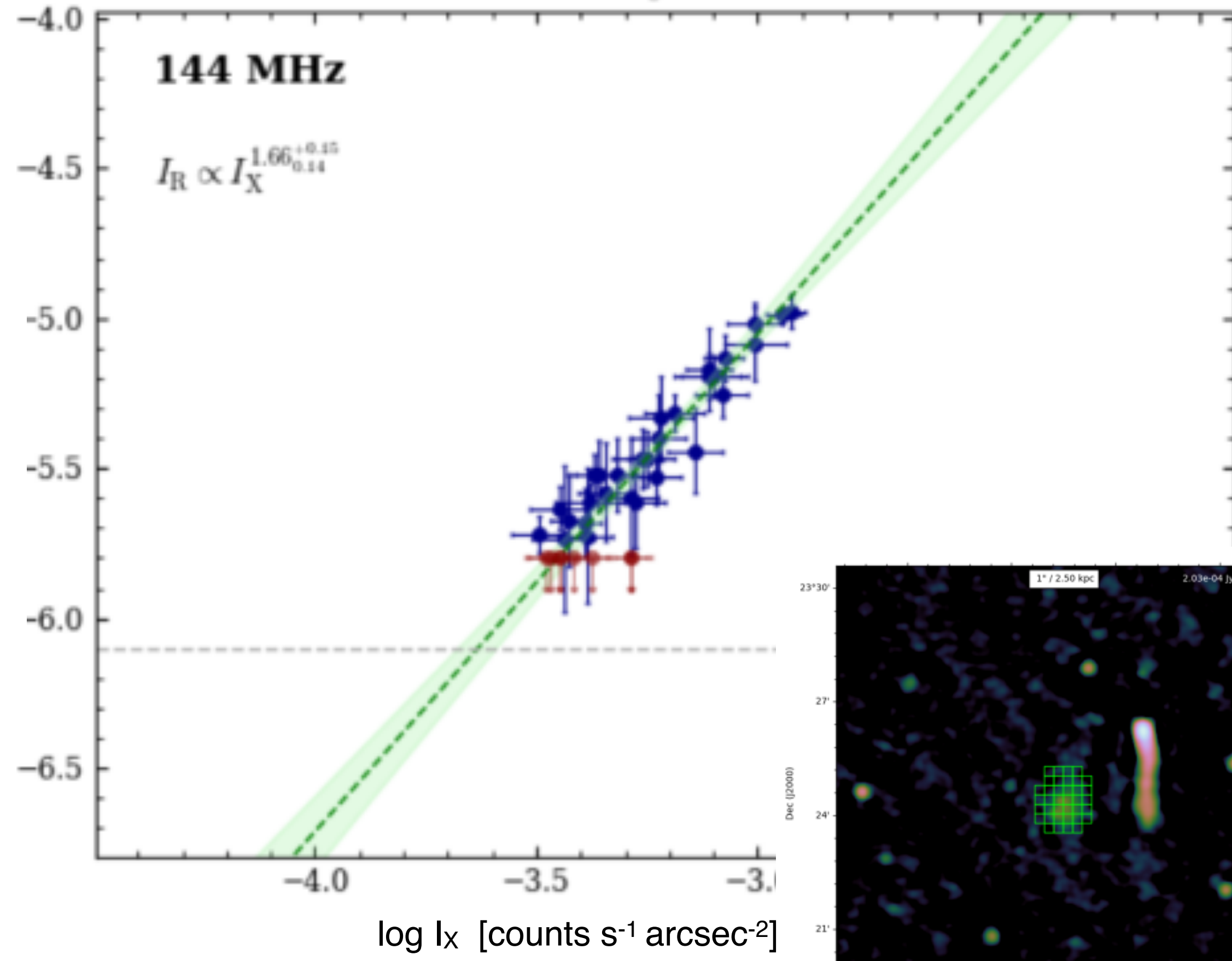
sub-linear

$$I_{R,halo} \propto I_X^{0.63}$$

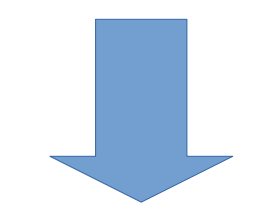
(incompatible with hadronic models)

Point-to-point correlation: *mini-halo emission*

$I_{radio} - I_{Xray}$ correlation

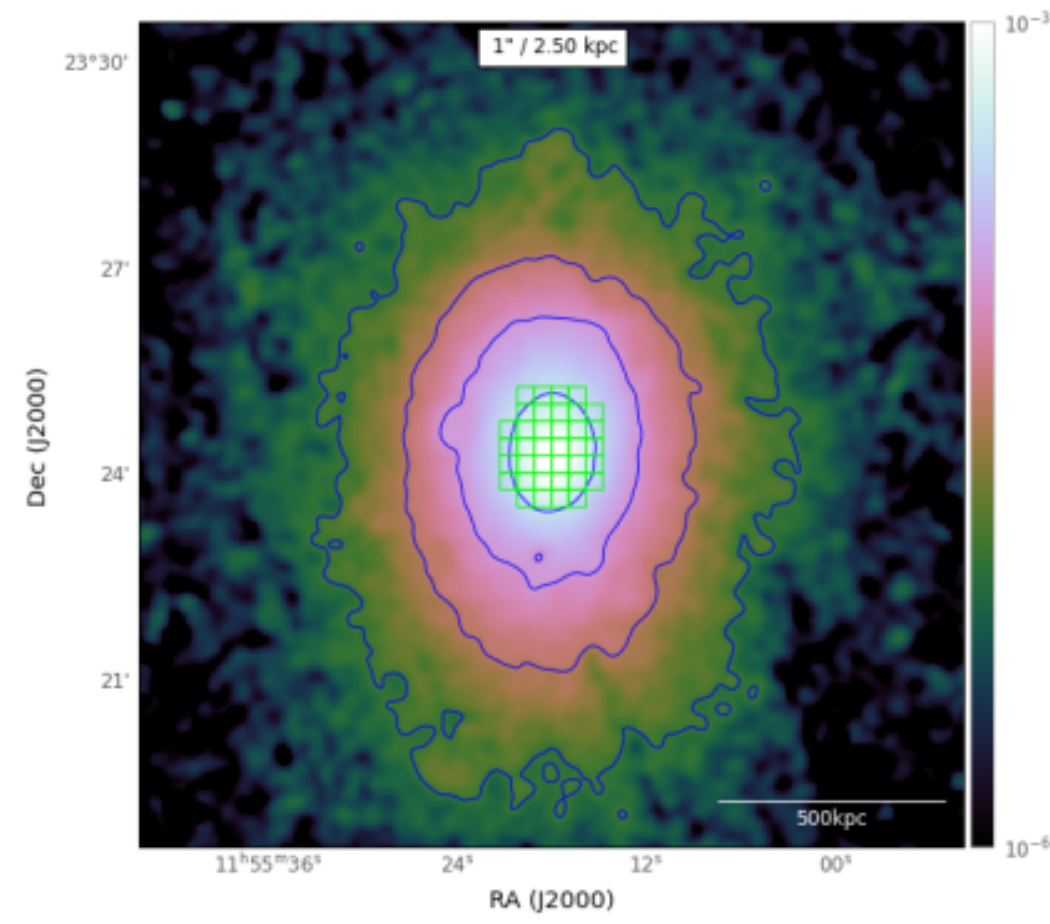
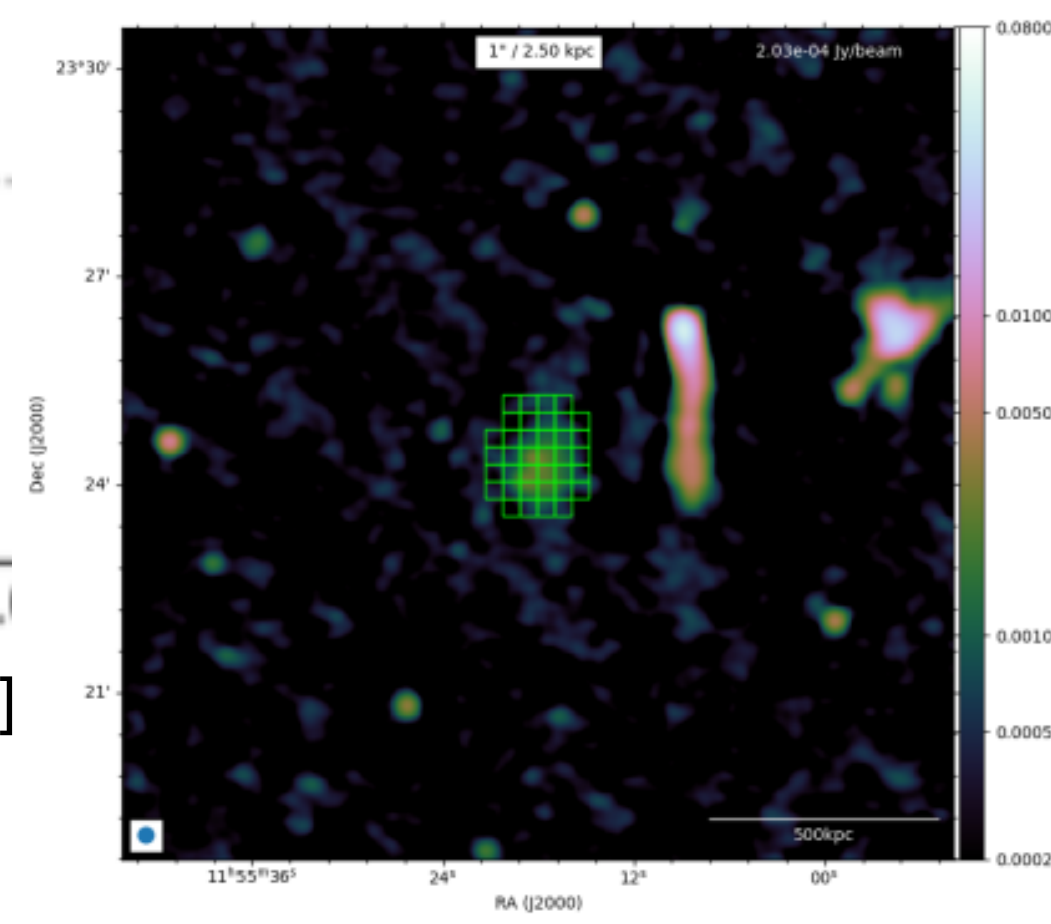


Mini-Halo	Grid	A	r_p
$I_R - I_X$	15'' × 15''	1.66 ^{0.16} _{0.13}	0.93



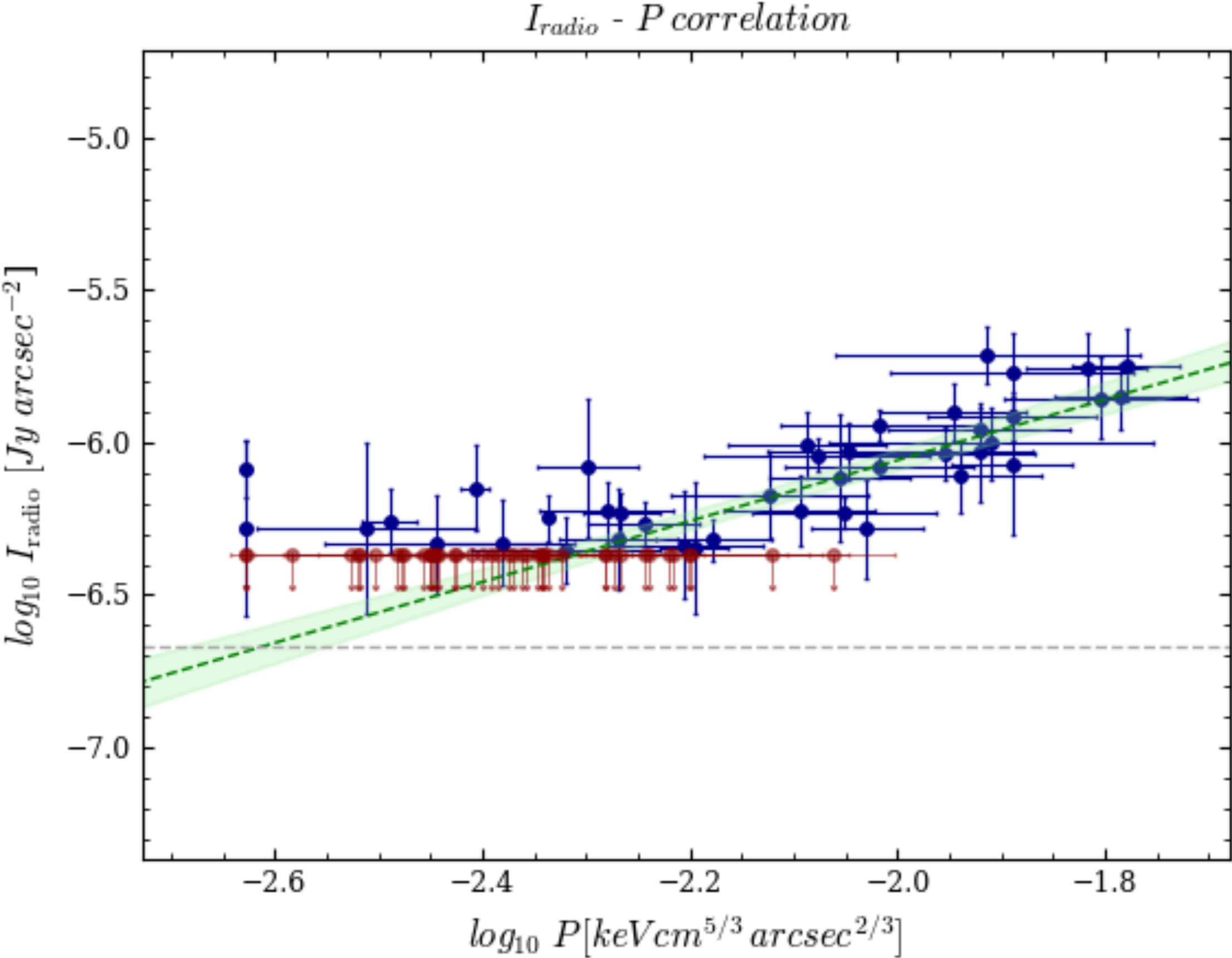
super-linear

$$I_{R,mini-halo} \propto I_X^{1.66}$$

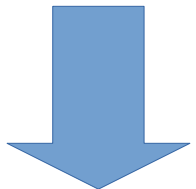


Further perspective: connection with other thermodynamical quantities

Point-to-point comparison between **radio** surface brightness and **pressure**



Halo	Grid	A	r_p
$I_R - P$	$35'' \times 35''$	$0.99^{0.13}_{0.12}$	0.78



$$I_{R,halo} \propto P^{0.99}$$

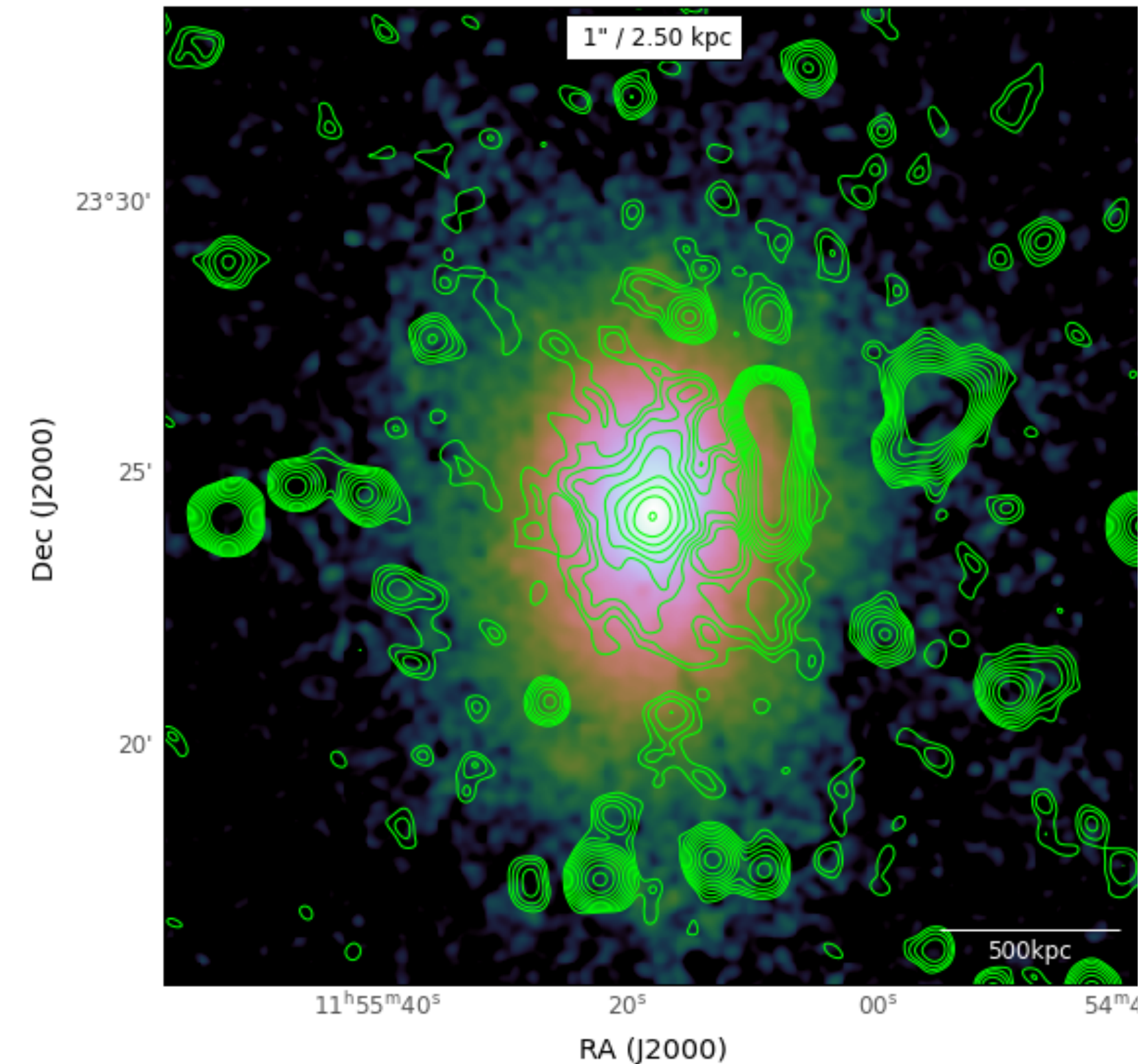
Summary:

- Multi-wavelengths study
 - using archival **XMM-Newton** data newly processed
 - imaging of new recent **LOFAR** data at 144MHz from LoTTS

- A1413 is not undergoing mergers and does **not have a disturbed morphology**. There are indications that at later time the cluster experienced some minor merger event → **not fully relaxed cool-core**

- This turbulent event has created the extended radio halo emission without destroying the cool core: cooling region < 90 kpc with
 - $t_{\text{central,cool}} \sim 6 \text{ Gyr} < 7.7 \text{ Gyr} \sim t_{\text{age}}$ (**weak-cool-core cluster**)

- A1413 hosts an extended low brightness halo emission superimposed with a central mini-halo emission. The **coexistence** of two different kinds of radio emission is suggested by
 - Different spectral index: $\alpha_{\text{mini-halo}} = 1.1 \pm 0.2$ vs $\alpha_{\text{halo}} > 1.6$
 - Different X-ray and radio surface brightness correlations
 - $$I_{R,\text{halo}} \propto I_X^{0.63} \text{ sub-linear} \quad \text{VS} \quad I_{R,\text{mini-halo}} \propto I_X^{1.66} \text{ super-linear}$$



A dark, starry night sky with a faint constellation outline in light blue. The word "Thanks" is written in a bold, white, sans-serif font in the center. The background is filled with numerous stars of varying colors and sizes, including a prominent bright orange star on the right and a small spiral galaxy in the lower center.

Thanks